Investigating Impacts of Wood Harvest on the Canadian Boreal Forest Carbon Store

Graham Clyne

A Thesis
In the Department of
Geography

Presented in Partial Fulfillment of the Requirements
For the Degree of
Master of Geography
at Concordia University
Montréal, Québec, Canada

June 2023

CONCORDIA UNIVERSITY
School of Graduate Studies

This is to certify that the thesis prepared

By: Graham Clyne

Entitled: Investigating Impacts of Wood Harvest on the Canadian Boreal Forest Carbon Store

and submitted in partial fulfillment of the requirements for the degree of

Masters of Science (Geography)

complies with the regulations of the University and meets the accepted standards with respect to originality and quality.

Signed by the final examining committee:

_____ Chair
Angela Kross

_____ Examiner
Damon Matthews

_____ Examiner
Andrew MacDougall

_____ Thesis Supervisor(s)
Damon Matthews

_____ Thesis Supervisor(s)

Approved by _____
Craig Townsend Chair of Department or Graduate Program Director

_____
Pascale Sicotte Dean of Faculty

Abstract

Investigating Impacts of Wood Harvest on the Canadian Boreal Forest Carbon Store

by Graham CLYNE

Earth System Models provide important insight into global climate dynamics. These models often require large computational resources to run, inhibiting accessibility and exploration of a wide range of climate-related scenarios. Machine learning can help by creating an emulation of an aspect of an ESM to enable less expensive scenario simulation. I use a Long Short-Term Memory model to emulate forest carbon dynamics in the Community Earth System Model 2 in order to understand the impact of wood harvest on carbon stocks in the Canadian Boreal forest. To validate the emulation, I use available external datasets that explicitly quantify carbon stocks in soil and above-ground biomass. The emulation can predict CESM2 several carbon stock variables accurately (0.89 R^2 Score) and can be explained with important climatic relationships. I then create land-cover scenarios to simulate no wood harvest for the years 1984-2019. These scenarios show that 584 Mt C were lost to wood harvest over this period, with an additional 172 Mt C attributed to regrowth from wood harvest over the same period. The LSTM model I use in this study provides a more flexible approach to investigating land-use change impacts on carbon stocks by harnessing the power of both machine learning models and process-based ESMs. This approach can help understand land-use change scenarios that are not considered in large inter-model comparison efforts.

Acknowledgements

This work would not have been possible without my supervisor, Dr. Damon Matthews, who has changed my life forever by agreeing to guide me through this degree. I am also eternally grateful for the guidance provided by my lab mate, Mitchell Dickau, without whom I would never even have applied for the program, let alone finish it. I would also like to acknowledge and thank Sydni Jackson, who always helped me stay focused, calm, collected and full of joy.

Contribution of Authors

Dr. Damon Matthews provided general guidance for all work completed in this thesis.

Contents

List of Figures

List of Tables

List of Abbreviations

CESM2	Community Earth System Model 2
LAMSE	Latitude-adjusted Mean Squared Error
LSTM	Long short-term memory
AGB	Above-ground biomass
BGB	Below-ground biomass
DOM	Dead Organic Matter
NFIS	National Forest Information System
NTEMS	National Terrestrial Ecosystem Monitoring System
LiDAR	Laser imaging,detecting and ranging
MSE	Mean-squared error
IG	Integrated Gradients
ERA5	ECMWF Re-Analysis
GHG	Green-house Gas
ESM	Earth System Model
ML	Machine Learning
LULCC	Land use and Land Cover Change
FAO	Food and Agriculture Organization
NbS	Nature-based Solutions
GCB	Global Carbon Budget
HWP	Harvested Wood Products

Chapter 1

Introduction

Over the past several decades, the IPCC has consistently reported a sharp and consistent increase in CO2 concentration in the atmosphere, entirely attributed to human activities (Arias et al., 2021). Increased atmospheric CO_2 concentrations cause increased temperatures that create a wide variety of climatic impacts, such as increased frequency of natural disasters and increased sea level (Arias et al., 2021). As per the Paris Agreement, the global community has agreed to attempt to keep the temperature increase to between 1.5°C and well below 2°C above pre-industrial levels (Arias et al., 2021). By limiting temperature increases to this level, it is thought that many of the negative effects of climate change will be manageable (Arias et al., 2021). The temperature increase has an almost linear relationship to cumulative CO2 emissions and it is, therefore, important to limit total CO2 emissions to reach the Paris Agreement's targets (Matthews et al., 2009).

Forests are vital ecosystems that provide numerous benefits, including carbon sequestration and storage. Modelling forest carbon dynamics is a crucial tool for predicting the future of forests and their role in mitigating climate change. Land Use and Land-Cover Change (LULCC) are anthropogenic actions taken to alter land cover and have a large impact on forest carbon dynamics. LULCC contribute significantly to the uncertainties in quantifying forest carbon stocks (Friedlingstein et al., 2022). By quantifying wood harvest impacts on carbon stores via several different methods, this uncertainty can be reduced. The IPCC encourages consideration of differences in methods to understand better net emissions from land sectors (Joeri Rogelj et al., 2022).

Nature-based solutions (NbS) are tools that leverage natural solutions to climate change mitigation (Griscom et al., 2017). Forest management is one such tool, and by further understanding wood harvest impact this NbS can be implemented more effectively. Canada's forest is a large carbon sink due to the large amount of vegetation (Kurz et al., 2018). This is a good opportunity to utilize NbS, as low-cost strategies can be implemented with high impacts (Griscom et al., 2017). A significant amount of carbon is lost due to wood harvest each year, and with further understanding mitigation efforts can be more effectively implemented (Kurz et al., 2018).

The aim of this thesis is to develop and apply a machine learning model that accurately captures the dynamics of forest carbon storage as represented by a comprehensive ESM. Specifically, this thesis will focus on developing an ML model that

represents forest carbon dynamics to be able to understand impacts of wood harvest on forest carbon stocks in the Canadian Boreal forest. This approach will enable knowledge from large climate models to be applied to climate-related scenarios without having to spend the computational resources often required to use a large climate model.

In this thesis, I set out to advance our understanding of the impact of wood harvest on forest carbon and contribute to the development of more effective forest management and climate change mitigation strategies. By combining process-based climate models with learning algorithms, I look to make a meaningful contribution to the ongoing efforts to mitigate climate change.

Chapter 2

Literature Review

2.1 Impacts of LULCC and Associated Uncertainties

Fossil fuels and Land Use and Land-Cover Change (LULCC) are the two most significant sources of anthropogenic CO2 emissions (Canadell et al., 2021). LULCC is any practice that changes land cover, including creating or abandoning cropland, afforestation, logging, and urbanization (Friedlingstein et al., 2022). Disturbance events release carbon back into the atmosphere, decreasing the carbon storage of the affected forest (Anderegg et al., 2020). Reforestation of grazing areas in previously forested areas and further avoidance of deforestation, both types of LULCC, are two practices with a large potential for climate change mitigation (Griscom et al., 2017). Even though there is potential to increase carbon sequestration through more carbon-conscious forest management, natural climate solutions must be used in tandem with solutions that reduce fossil fuel emissions to net zero as it is not guaranteed that the carbon sequestered from natural climate solutions will be permanent (Matthews et al., 2022).

Determining particular effects of LULCC, and wood harvest in particular, on carbon stores has many uncertainties. Intuitively, both Wang et al. and a 2022 study of British Columbia forests conducted with inventory data and carbon models found that logging had a negative effect on carbon stocks (DellaSala et al. 2022, Wang et al. 2021). However, how a forest is defined can play a large role in determining the different effects of LULCC. The Food and Agriculture Organization (FAO), a large source for inventory-based studies (which are also used in the Global Carbon Budget analysis), assembles over 90% of its data from countries where reports are inconsistent in method, scope and definition (MacDicken, 2015). The FAO also defines deforestation as the removal of trees where no regrowth occurs, but it is not considered deforestation if the forest is expected to grow back with or without silviculture (Chazdon et al., 2016). This definition could be misleading when trying to understand climatic impacts, as rates of carbon sequestration vary over the life of a tree (Chazdon et al., 2016). These definitions can also undervalue adjacent processes to tree growth. Researchers found that carbon content in soil decreased after a harvest event for several decades until carbon sequestration from regrowth outweighed carbon loss from decomposition (Johnson et al., 2010).

The 2022 Global Carbon Budget, the most well-known global effort to quantify yearly anthropogenic carbon emissions and natural carbon exchange with the land and ocean carbon systems, assigns high uncertainty (determined by the standard deviation of the ensemble of Dynamic Global Vegetation Models, process-based models that simulate vegetation dynamics) to the carbon flux of the terrestrial land sink and LULCC emissions (Friedlingstein et al., 2022). Pongratz et al. concluded that differences in approaches to modeling terrestrial carbon stores and LULCC - setup of model parameters, different underlying LULCC data sources, and different complexity of LULCC representation in models - is a major source of uncertainty for the Global Carbon Budget (Pongratz et al., 2021). For example, both the Global Carbon Budget and Pan et al. found over 50% uncertainty in the emissions from global land-use change from 1990-2000 (4.8GtC +/- 2.6 compared with 5.5GtC +/- 2.6, Friedlingstein et al. 2022, Pan et al. 2011).

2.2 Afforestation and Nature-Based Solutions

Nature-based Solutions (NbS) have been recently highlighted as tools that can provide potential mitigation for the impacts of future climate change (Griscom et al., 2017). Forest management is one such method of NbS, and is one of the most promising methods to increase carbon sequestration in Canadian forests (Wang et al., 2021). Afforestation, the practice of creating forests where there was no forest, would generate an increased carbon sequestration associated with the increased amount of forests. While the effect of afforestation on the carbon cycle is somewhat clear (i.e., promotes carbon uptake), the effect of afforestation on global mean temperature is uncertain and locally specific. For instance, increasing forest cover reduces surface albedo and can cause regional warming which offsets the climate benefit of carbon sequestration (Canadell et al. 2021, Pongratz et al. 2021). Reforestation is a similar process to afforestation, but instead creates forest where there was previously forest (Pongratz et al., 2021). Pongratz et al. identify that further investigation on the effects of particular LULCC practices on the climate is needed, noting that this is becoming more feasible as datasets that distinguish LULCC practices are more readily available (Pongratz et al., 2021).

2.3 Canada's Forests and Carbon Stock Estimation

Being able to approximate carbon storage accurately is crucial to understanding the historical and future impacts of wood harvest. Estimations of the terrestrial carbon flux in the 2022 GCB includes several Dynamic Global Vegetation Models as well as bookkeeping methods (a tally of carbon emissions and sequestrations from a historical base level). The terrestrial carbon flux has two components that are influenced by human factors: the terrestrial land sink (the portion of anthropogenic

CO2 emissions being sequestered by the land biosphere), and land-use change emissions. The terrestrial land sink is composed of elements that contribute to increased land carbon sequestration in response to anthropogenic influence on the carbon cycle. Depending on the region, these could include a longer growing season and CO2 fertilization – the enhancement of photosynthesis that results from elevated atmospheric CO2 concentrations (Friedlingstein et al., 2022). The land-use change emissions are determined by human-induced factors, such as logging, agriculture and deforestation (Friedlingstein et al., 2022). The GCB does not explicitly quantify the effects of individual LULCC, instead aggregating all land-use practices into one group (Friedlingstein et al., 2022). This aggregation provides a yearly estimate of the net global terrestrial carbon flux, although the GCB does not provide more regionally granular data (Friedlingstein et al., 2022).

Canada's forests are deemed "managed" or "unmanaged" based on the occurrence of forestry activities that include wood harvest and silviculture practices (Canada 2023,Kurz et al. 2018). Canada's managed forest is 225.52 million hectares and spans all provinces and territories, with the exception of Nunavut (Canada, 2023). The managed forest designation is used for GHG inventories for the National Inventory Report and submission to the United Nations Framework Convention on Climate Change (Canada, 2023). Canada's forest is also sometimes divided by ecozone. Canada is divided into several ecozones that represent different ecological areas (Wiken et al., 1996). Each ecozone designates an area of cohesive biophysical traits and biome (Wiken et al., 1996). Canada's managed forest does not include several of Canada's ecozones, as there is no harvest activity in several of the biomes due to a lack of forest cover (Canada, 2023).

Several studies investigate above-ground biomass (AGB, biomass stored in the region above-ground, i.e. stems, bark, leaves etc. Distinct from below-ground biomass) and wood harvest impacts in Canada's forests using some combination of the study areas described above. Canada uses the Carbon Budget Model of the Canadian Forest Sector (CBM-CFS3) to model the forest carbon dynamics for Canada's managed forest (Kurz et al. 2018,Canada 2023). This is a yield data driven regional climate model that focuses on forest carbon dynamics and can represent anthropogenic effects on forests (Kurz et al., 2018).

Kurz et al. found that forest that was affected by anthropogenic activities after the year 1990 was an estimated net sink of between 134-163 Mt CO_2 per year from 1990 to 2016 (Kurz et al., 2018). This includes activities such as clear cutting, partial harvest and burning of forest residues and reforestation (Kurz et al., 2018). The CBM-CFS3 has been validated externally using ground plot data from the National Forest Inventory, and found high agreement with observations (Kurz et al., 2013).

As more observational data becomes available, approaches incorporating this data are becoming more common (Pongratz et al., 2021). Eddy-covariance towers have also been very important for quantifying local carbon exchanges between land and the atmosphere, but have difficulty when trying to calculate carbon stocks of larger areas (Schulze et al., 2021). Another study that quantifies AGB in all of

Canada's ecozones with a combination of LiDAR and satellite imagery found that 1.73 Gt C of above-ground biomass carbon were lost due to wood harvest between the years 1984 and 2016 (Wulder et al., 2020). This is approximately 50 Mt C per year over the period, which is significantly lower than the estimate in Kurz et al. This study, unlike Kurz et al., looks at both the managed and unmanaged forests of Canada, although by definition, the vast majority of wood harvest activity occurs in the managed forest (Wulder et al., 2020). Wulder et al. employ several land-cover datasets provided by the National Forest Inventory that have been recently developed and are not employed in Kurz et al. (Wulder et al. 2020, Kurz et al. 2018). Wulder only considers AGB and uses data-driven approaches, opposed to Kurz et al. who account for the whole forest carbon store (AGB, BGB, DOM etc.) using a yield data-driven model (Kurz et al., 2018). Pan et al. compose a global image of forest carbon and find that for the years 1990-2007, 22 +/- 7 Mt C per year were attributed to wood harvest in Canada (Pan et al., 2011). These numbers are based on simulations from the CBM-CFS3 (Pan et al., 2011). There is clearly significant disparity in estimations of impact on forest carbon stocks across studies.

Significant differences are also found in comparisons in total AGB. Wang et al. combines LiDAR data with Landsat satellite imagery to estimate above-ground biomass (AGB) in North-Western North America (Wang et al., 2021). Wang et al. find for the year 2014, the total AGB in the Boreal Plain (an ecozone in central Canada) was 1763 Mt C. For the same area, Wulder et al. find the total AGB to be 3324 Mt C (Wulder et al., 2020).

There is strong agreement from this myriad of methods that the canadian boreal carbon store has increased over the last few decades (Pan et al. 2011,Tagesson et al. 2020,Friedlingstein et al. 2022,Wang et al. 2021). The cause for this increase is still in debate, but its largest driver is widely attributed to CO2 fertilization (Tagesson et al., 2020). Initial carbon pool size, nitrogen deposition and climate are also important factors, but the size of the impact from these factors is variable depending on the model (Huntzinger et al., 2017). The Canadian boreal forest was the largest global terrestrial carbon sink from 1992-2015, and the contribution of the Canadian boreal forest to the global carbon sink increased over that period (Tagesson et al., 2020).

Although there is agreement that the boreal carbon store has increased, the quantity of the carbon store and rate of increase is still uncertain. Wang et al. found that the Coupled Model Intercomparison Project 6 (CMIP6) models (the ensemble of models used in the GCB) routinely over-estimated AGB and net biome productivity (the net carbon accumulation of an ecosystem) when compared to the observational method employed (Wang et al., 2021). The source of this discrepancy is unclear. Wang et al. use a scaling relationship to convert total vegetation carbon from climate models to AGB to be able to compare observational results (Wang et al., 2021). Using AGB to understand the total carbon vegetation in an ecosystem, as in Wang et al., can potentially overlook other forest carbon dynamics. When carbon allocation to AGB is compared to net ecosystem productivity (NEP, the same as net biome productivity), the carbon allocation remains stable while the NEP is highly variable

(Pappas et al., 2020). While this may explain some of the discrepancies outlined in the above studies, further study is needed to reduce uncertainty.

2.4 Climate Models and Machine Learning

To understand the past and future climate, numerical models are used (Arias et al., 2021). Climate models that are based on mathematical equations that represent physical processes are known as process-based models (Danabasoglu et al., 2020). The CBM-CFS3 used in Kurz et al. contains elements that are process-based, such as dead organic matter (DOM - dead fall, slash etc.), but is predominantly a yield data driven climate model (Kurz et al., 2009). Yield data driven models take input on wood volume derived from stand age and type, as well as spatially explicit maps of land-use change and return variables that describe carbon dynamics (Kurz et al., 2009). Instead of attempting to recreate physical processes, the CBM-CFS3 primarly relies on yield curves over time to describe changing forest dynamics (Kurz et al., 2009). Numerical models (both process-based and yield-curve models) can be both simple and complex representations of the climate. For example, the FAIR model only models the atmospheric concentration and effective radiative forcing of greenhouse gases (Smith et al., 2018). The model is tuned to approximate future projections of larger models and is used to model thousands of scenarios (Smith et al., 2018). On the other hand, the Community Earth System Model 2 represents a large number of climatic processes in Earth's climatic system (Danabasoglu et al., 2020). The latter requires significant computational resources to run, and is often run with large computer clusters (Watson-Parris, 2020).

As a way to circumvent this large computational cost, climate model emulations, also known as surrogate models, have been used (Watson-Parris, 2020). The Finite Amplitude Impulse Response model is considered a climate model emulation, as it attempts to reproduce results used in more complex climate models (Smith et al., 2018). Recently, machine learning has been used as a tool to complement process-based climate models (Watson-Parris, 2020). Climate models have many parameters that represent different physical processes. For example, the Community Land Model 5 (the land component of the CESM2) has a parameter that represents the dimension of leaves in the direction of windflow (Dagon et al. 2020,Lawrence et al. 2019). This parameter can be tuned to best match historical observations, and machine learning can aid in finding the best value by learning the relationships in the climate model and permuting many different parameter values (Dagon et al., 2020). With this emulation, they were able to quickly run many simulations of the model using different values of parameters to find optimal values that best fit observations (Dagon et al., 2020). These optimal values were then used in the climate models to help future predictions. Machine learning can also help in creating new parameterizations for processes not fully understood, or processes that resolve at a resolution smaller than the resolution of the climate model (Rasp et al., 2018). ML is

also frequently used for down scaling resolution of climate models to provide regional climate predictions (Doury et al., 2022). Doury et al. train a neural network (a machine learning algorithm that optimizes a function using gradient descent) with several climatic variables from a regional climate model (Doury et al., 2022). Once the model is trained, they apply it to a global climate model with much lower resolution but wider spatial coverage. With this model, they are able to get a finer resolution of climate without having to run a process-based climate model at a finer resolution (Doury et al., 2022).

There is precedent for incorporating machine learning techniques to work with both data from climate models and real-world observations. In both Doury et al. and Dagon et al., only climate model output is used. Machine learning can learn an approximation of the processes behaviour through observed data, and couple this approximation to a climate model (Rasp et al., 2018). One study extended prediction lead times of El Niño/Southern Oscillation to one and a half years by supplementing observational weather data with data generated from a climate model and using deep learning techniques (Ham et al., 2019). This methodology of mapping simulated output to observational data goes by several names (such as hybrid modeling, process-guided learning, climate model emulation, and process-informed learning) and can be used in a wide range of domains in environmental science (e.g. (Gibson et al., 2021),(Hanson et al., 2020)).

Recently there have been significant contributions to the study of emulating process-based climate models with machine learning. Climatebench was a recent effort to provide a benchmark for data-driven climate modelling efforts (Watson-Parris et al., 2022). Watson-Parris et al. defined a set of metrics to help guide emulator evaluation, and applied their metrics to a neural network that performed well when compared with other climate models (Watson-Parris et al., 2022). ClimaX, more recently, was an attempt to create a more general emulation (a "foundation model") that can perform multiple climate related tasks by emulating an ensemble of climate models (Nguyen et al., 2023). Nyugen et al. trained a machine learning model using output from several process-based climate models in order to perform weather forecasting, downscaling and long-range climate prediction (Nguyen et al., 2023). Graphcast, a medium-range weather forecasting model based on graph neural networks, outperformed other state-of-the-art process-based weather models (Lam et al., 2022).

Long Short-Term Memory models are a special case of a neural network that has been shown to work well with climatic time series data (Granata and Di Nunno, 2021). In Granata et al., researchers use several observed climatic variables that inform evapotranspiration in Florida. They then applied LSTMs to estimate 1-day ahead predictions of evapotranspiration using time series of the climatic variables (Granata and Di Nunno, 2021). By using a time series of variables, the neural network learned a more holistic picture of the climate in question (Granata and Di Nunno, 2021).

Explainability of machine learning algorithms is important when working with

climatic data, as the how is often just as important as the why (Watson-Parris, 2020). Neural networks are considered a "black box", an algorithm where the process that it learns is not visible (Mamalakis et al., 2022). To help understand neural networks, Sundararajan et al. used a method called Integrated Gradients (IG), which determines the importance of features by taking the integral of the model's gradients along a straight path from a baseline (a zero vector, which in this case is the mean of the normalized data) to the input (Sundararajan et al., 2017). This method helps understand what the model has learned by attributing importance to the different input features (Sundararajan et al., 2017).

To learn better impacts of wood harvest, these machine learning techniques can learn forest carbon dynamics. This understanding can be applied to real-world data to explore a different method of forest carbon stock estimation. In this research I will use machine learning with output from climate models to learn a comprehensive representation of forest carbon dynamics. I will then create two wood-harvest scenarios: one that considers no wood harvest occurred from 1984-2019, and one that considers no regrowth occurred after wood harvest for the same period. Using both of these scenarios, I apply the machine learning model trained on climate model data to estimate the impact of wood harvest on forest carbon stocks.

Chapter 3

Manuscript

3.1 Abstract

Earth System Models provide important insight into global climate dynamics. These models often require large computational resources to run, inhibiting accessibility and exploration of a wide range of climate-related scenarios. Machine learning can help by creating an emulation of an aspect of an ESM to enable less expensive scenario simulation. I use a Long Short-Term Memory model to emulate forest carbon dynamics in the Community Earth System Model 2 in order to understand the impact of wood harvest on carbon stocks in the Canadian Boreal forest. To validate the emulation, I use available external datasets that explicitly quantify carbon stocks in soil and above-ground biomass. The emulation can predict CESM2 several carbon stock variables accurately (0.89 R^2 Score) and can be explained with important climatic relationships. I then create land-cover scenarios to simulate no wood harvest for the years 1984-2019. These scenarios show that 584 Mt C were lost to wood harvest over this period, with an additional 172 Mt C attributed to regrowth from wood harvest over the same period. The LSTM model I use in this study provides a more flexible approach to investigating land-use change impacts on carbon stocks by harnessing the power of both machine learning models and process-based ESMs. This approach can help understand land-use change scenarios that are not considered in large inter-model comparison efforts.

3.2 Introduction

Earth System Models (ESMs) simulate climate by representing climatic processes mathematically to generate estimations of past and future climates. ESMs can be used to understand impacts of climate change and mitigation efforts to combat climate change. These models represent a large number of climatic processes globally and require considerable amounts of computational resources to run. In order to reduce these demands of an ESM, creating an emulation of an ESM has proven to be a useful complement to process based modelling. Climate model emulation has been popular for several decades as a method to circumvent the large computational resources needed to run an ESM (Osborn et al., 2006). These climate emulators have

been used in the IPCC to help simulate future climate scenarios, although detailed climate and carbon cycle dynamics are still represented with ESMs (Canadell et al., 2021). Some emulators use many parameters that represent different climatic processes, and are tuned to match the output of larger ESMs (Smith et al., 2018). Such emulators can then be run thousands of times at a fraction of the computational resource in order to explore many different future climate scenarios (Smith et al., 2018).

Machine learning has proven effective at emulating some climatic processes (Rasp et al., 2018) (Ham et al., 2019) (Nguyen et al., 2023). Forest carbon dynamics are one such group of processes. Simulating these processes is often done with an ESM, and is used to help understand global carbon dynamics (Friedlingstein et al., 2022). There is also a rich practice of estimating forest carbon through remote sensing, often using some combination of lidar, allometric equations and satellite imagery (Wulder et al., 2020). These methods focus on estimating above-ground biomass (AGB, the amount of living biomass above ground, shrubs, trees, leaves etc), with far less research aimed at estimating soil carbon or below-ground biomass due to a lack of observations (Sothe et al., 2022). Using machine learning (ML) within the field of Earth Sciences has become increasingly popular to help estimate and explain climatic processes (Watson-Parris, 2020). For example, ML has been used to gain at-scale estimations of soil carbon and improve medium-range weather forecasting (Sothe et al. (2022),Lam et al. (2022)).

In this work I use machine learning to emulate the Community Earth System Model 2 (CESM2) simulation of above- and below-ground carbon stocks. I first emulate the CESM2 model using a Long Short-Term Memory (LSTM) model, which excels at interpreting time series data. I then validate the LSTM model by comparing the emulation to available data sources. I aim to train a machine learning model on climate model data that is internally consistent. Once the emulation accurately represents the selected processes, I apply this emulation to a land-cover scenario that investigates the historical impacts of wood harvest in the Canadian Boreal forest. The land-cover scenario is based on principles inspired by Nature-based Solutions (NbS), actions or practices that protect or restore natural habitats (Griscom et al., 2017). NbS have been recently highlighted as tools that can provide potential mitigation for the impacts of future climate change (Griscom et al., 2017). Forest management is one such method of NbS, and is one of the most promising methods to increase carbon sequestration in Canadian forests ((Wang et al., 2021) (Griscom et al., 2017)). By simulating several forest management scenarios, this research will provide methods to inform actionable mitigation policy.

3.3 Materials and Methods

3.3.1 Study Area

Canada is divided into several ecozones that represent different ecological areas (Wiken et al., 1996). In this research I focused on three ecozones: the Boreal Plain, the Boreal Shield and the Boreal Cordillera. These three ecozones share differing biophysical traits but have similar vegetation, primarily covered in forest (Wiken et al., 1996). Canada's forests are deemed "managed" or "unmanaged" based on the occurrence of forestry activities that include wood harvest and silviculture practices ((Canada, 2023) (Kurz et al., 2018)). Canada's managed forest is 225.52 million hectares and spans all provinces and territories, with the exception of Nunavut (Canada, 2023). The managed forest designation is used for GHG inventories for the National Inventory Report and submission to the United Nations Framework Convention on Climate Change (Canada, 2023). The three ecozones in this research are all within Canada's managed forest and represent a significant portion of Canada's forest cover (Wiken et al., 1996). I chose these three ecozones to provide a coherent and unified study area composed of similar ecosystems and climates. These boreal regions are dominated by tree cover and have longer winters and shorter summers (Wiken et al., 1996).

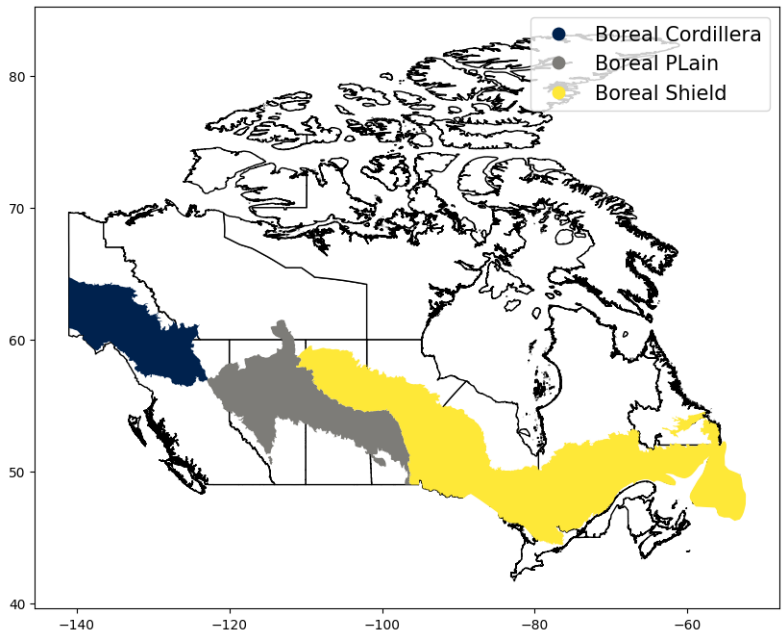

FIGURE 3.1: Study area used for training and harvest scenario.

Ecozone	Forest Area (kha)
Boreal Cordillera	19,116.46
Boreal Plains	38,454.65
Boreal Shield	131,274.73
Canada	361,732.00

TABLE 3.1: Area of forest cover (kha) in the ecozones used in this study. Last line is total forest cover in Canada.

3.3.2 Data Sources

The climate model data I used to train the ML model comes from the CESM2 (Danabasoglu et al., 2020). The CESM2 is a coupled climate model that comprises several smaller modules representing particular physical processes, such as ocean dynamics or ice dynamics. The land climate model is called the Community Land Model 5 (CLM5). The CLM5 represents several land-carbon cycle dynamics, notably processes related to the nitrogen cycle, fire, CO_2 fertilization, permafrost and peatlands (Lawrence et al., 2019). The CLM5 represents many LULCC processes such as wood harvest (by mass) and agricultural management (Lawrence et al., 2019). The CLM5 adheres to a land-use change dataset, the LUH2, to determine what land-cover class is replaced by wood-harvest (David Lawrence et al., 2018). The Coupled Model Intercomparison Project (CMIP6), an organization aimed at facilitating climate model comparison, provides standardized variables as experiments for public use. The experiment "historical" is used as a control for several experiments in the CMIP6, and I used it here as input data (Danabasoglu et al., 2020). The historical experiment simulates recent (1850-2014) climate. I included seven variants of this experiment in the training data, where each variant was run with different initial forcings. This provides approximately 600,000 data points at a resolution of 100 km^2. I used six input variables: surface pressure, soil temperature, percentage of tree cover, summer near-surface air temperature, winter near-surface air temperature and precipitation (See Table 2).

To train the LSTM, I aggregated model output from CESM2 to a yearly temporal resolution to match the temporal resolution of the land-cover classes. I then aggregated the data to the lowest spatial resolution, that of the CESM2 (.9x1.25 degree finite volume grid, approximately 100 km^2). I then converted this data to time series data with a 30-year rolling window. All input data is scaled to a standard normal distribution.

After training the ML model, I used a combination of National Terrestrial Ecosystem Monitoring System (NTEMS) and ERA5 reanalysis land monthly means to create a dataset that I used to represent the climate of the study areas without the bias of the climate model (Muñoz-Sabater et al., 2021). The NTEMS dataset provides land-cover classification from 1984-2019 and uses the EOSD land cover hierarchy to provide 12 land-cover classes at 30m resolution and provides the treeFrac variable

data (Hermosilla et al., 2018). These data products provide a country-wide consistent land use and land-cover change map for the study period. The ERA data provides the rest of the climatic variables. I aggregated this data to the $100 km^2/year$ resolution used in the CESM2 and used a 30-year rolling window. This dataset will be referred to as ERANFIS in this study.

To validate the ERANFIS dataset, I used two available datasets that provide spatially-explicit maps of AGB carbon. Another product from NTEMS, a 2015 AGB dataset, approximates AGB carbon using lidar and LANDSAT satellite imagery (Matasci et al., 2018). Walker et al. use lidar and MODIS satellite imagery with regression models to estimate AGB carbon (Walker et al., 2022). I used both Walker et al. and Matasci et al. to validate the AGB carbon represented in ERANFIS. I used a dataset made from a collaboration between the World Wildlife Foundation and McMaster University that provides country-wide estimates for soil carbon above 1m depth at 250m resolution to validate the soil estimates of ERANFIS (Sothe et al., 2022). In the CESM2, above-ground biomass is defined as the sum of cLeaf, cOther and cStem. Both AGB and cSoilAbove1m are chosen for ease of comparison to other studies (see Results section). I used another product from NTEMS that provides a map of wood harvest events from 1985-2019 at 30m resolution to create wood-harvest scenarios (see Wood-harvest Scenario section, Hermosilla et al. (2016)).

3.3.3 Model Description and Metrics

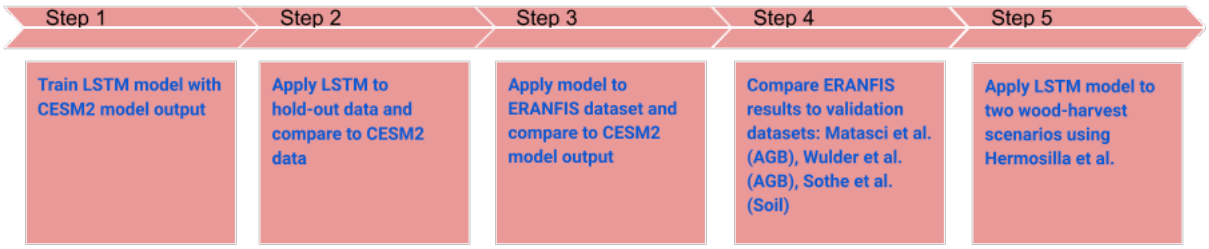

FIGURE 3.2: Flowchart of methods used in this study.

The ML model is an LSTM (long short-term memory) neural network with 4 layers and 256 hidden units in each layer. The inputs are 6 climate and land-cover variables: surface pressure, soil temperature, tree cover fraction, summer surface temperature, winter surface temperature and precipitation. The targets are 4 carbon stock variables: carbon mass in other vegetation, carbon mass in stems, carbon mass in leaves and carbon mass above 1m depth in soil pool. I chose these variables so that a dataset that represents real-world climate could be made (ERANFIS) and used to compare the model with other observable data. By only including one land cover class, tree cover, the ML model is the simplest and ideally most explainable version of the model possible. See Table 2 for further details. The model was trained for 16 hours on one v100 GPU.

CMIP6 Variable Name	**Description**	**Units**
ps	Surface pressure (not mean sea-level pressure) 2-D field to calculate the 3-D pressure field from hybrid coordinates	Pa
tsl	Temperature of soil, only consider top-layer (0-7cm)	K
treeFrac	Percentage of entire grid cell that is covered by trees	
tas_{JJA}	Near-surface (usually, 2 meter) air temperature for the months June, July and August	K
tas_{DJF}	Near-surface (usually, 2 meter) air temperature for the months December, January and February	K
pr	Precipitation, both liquid and solid phases	$kg/m^2/s$
cOther	Carbon mass in vegetation components other than leaves, stems and roots	kg/m^2
cStem	Carbon mass in stems	kg/m^2
cLeaf	Carbon mass per unit area in leaves	kg/m^2
cSoilAbove1m	Carbon mass in soil pool above 1m depth	kg/m^2

TABLE 3.2: Variable descriptions and units in CMIP6. Variables below the double line are target variables, with cStem, cLeaf and cOther making up above-ground biomass.

I used the following loss function, where $\cos(lat)$ is the latitudinal scaling factor to account for decreasing grid cell size, y is the target and $\hat{y}$ is the prediction:

$$LAMSE = \cos(lat) * \frac{\sum_i^n (y_i - \hat{y}_i)^2}{n} \tag{3.1}$$

To evaluate the model, I used the coefficient of determination, denoted R^2 and computed as follows (where SS_res is the sum of residual squares and SS_tot is the total sum of squares). This metric helps determine the amount of variation that can be attributed to the predictions:

$$R^2 = 1 - \frac{SS_{res}}{SS_{tot}} \tag{3.2}$$

3.4 Results

I first trained the model using the CESM2 model output. I trained the model with an 70/20/10 train/validation/hold-out split, with the data split spatially by grid cell. The units for the Latitude-Adjusted MSE (LAMSE) in Table 2 are the original units used in training, and have not been converted to Mt C. This ensures spatial scaling with the loss function is consistent. Table 3 shows the results from training the LSTM on the output from the CESM2 model. These numbers show the LSTM is capable of optimizing the loss function provided and can accurately predict values in the hold-out data.

	R^2	**LAMSE** (kg/m^2)
Training Data (70%)	.91	.11
Validation Data (20%)	.91	.20
Hold-out Data (10%)	.89	.35

TABLE 3.3: Evaluation metrics from model training. CESM2 data was split randomly by grid cell to compose each dataset. LAMSE is Latitude-Adjusted Mean Squared Error.

I compared the emulation applied to ERANFIS (the dataset created based on ERA5 reanalysis data and observed land-cover from NFIS) with the original output from the CESM2. There are significant differences between the two datasets although this is to be expected; while the climates are similar in aggregate, they differ from grid cell to grid cell (See the Supplemental Material section for comparisons of input data). We can see in Figures 3 and 4 that there are significant spatial differences between the carbon stocks estimated by ERANFIS and CESM2.

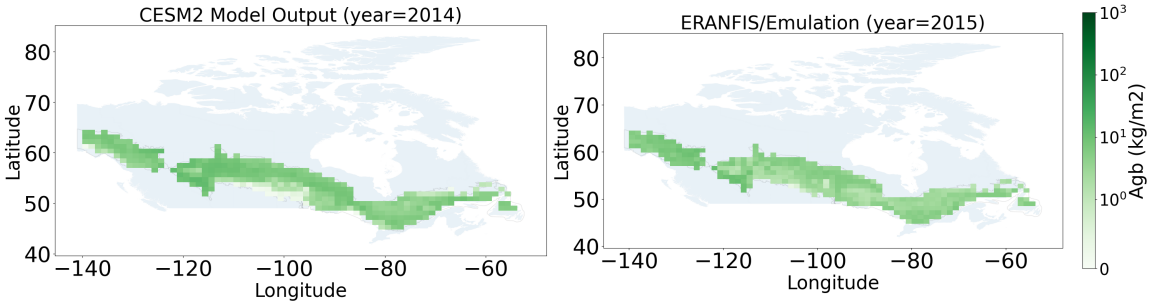

FIGURE 3.3: ERANFIS compared to CESM2 model output of AGB carbon.

I then compared ERANFIS to two different observation-based datasets that estimate AGB for the year 2015. The first dataset, from Matasci et al., is derived from the same land-cover data used in training (from NTEMS) and uses lidar with satellite imagery to generate country-wide estimates of AGB (Matasci et al., 2018). The second dataset (Walker et al., 2022) combines lidar with field measurements to make

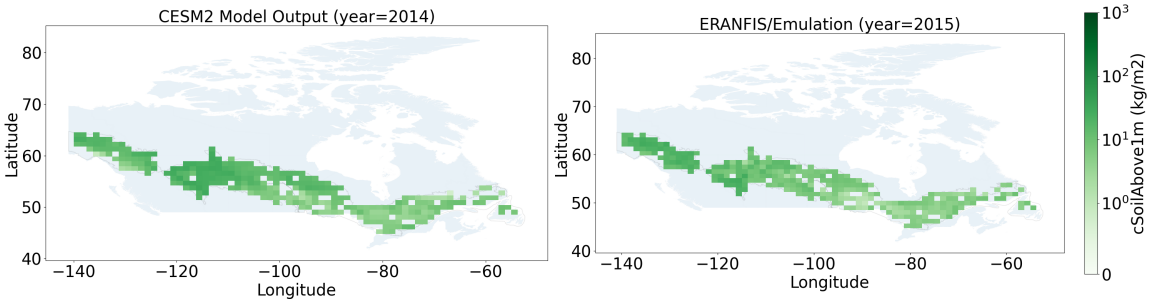

FIGURE 3.4: ERANFIS compared to CESM2 model output of soil carbon.

estimations of AGB globally (Walker et al., 2022). Data from 2014 is used for the CESM2, the last available year of data coverage. When comparing ERANFIS to observation-based datasets I used a non-spatial error estimator, the Mean-Squared Error (MSE), as the data is converted to Mt C for ease of comparison. We can see in Figure 5 that each dataset has noticeably different distributions of AGB. This is enumerated in Table 4 and Table 6, where we see that the R^2 of both the emulation and CESM2 is less than 0 in both cases (i.e., both compare worse than a dataset that only predicted the mean), although there is significant improvement with the emulation compared to the CESM2 model output. Table 5 shows the AGB totals where we can see that there is significant disagreement across all datasets. While the CESM2 estimates the highest values, ERANFIS displays the least variation in totals (the Boreal Cordillera and Boreal Plains are almost the same, see Supplemental Material for further discussion). Matasci et al. finds almost double the AGB that Walker et al. does (Matasci et al. (2018),Walker et al. (2022)).

Model	R^2	**Average LAMSE (kg/m^2)**
Matasci et al.		
ERANFIS	-0.47	9.63
CESM2	-1.85	18.76
Walker et al.		
ERANFIS	-8.27	8.33
CESM2	-21.19	19.94

TABLE 3.4: Evaluation metrics for ERANFIS and the CESM2 compared to both Matasci et al. and Walker et al. A negative R^2 score means the predictions are worse than predicting the mean.

Sothe et al. is used for comparison to cSoilAbove1m. We can see in Figure 5 that there are significant differences between the estimations. We can note that the scale of Sothe et al. is approximately 5 times greater, and reports more than 3 times the soil carbon when compared to the CESM2 and ERANFIS (See Table 5 and Table 7). Both ERANFIS and CESM2 perform equally poorly when compared to Sothe et al.

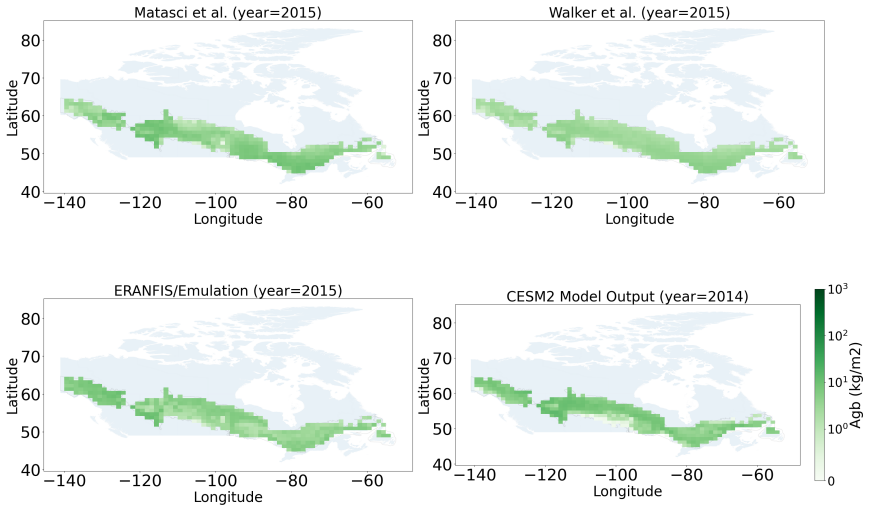

FIGURE 3.5: Spatial visualization of AGB comparison. The top row shows the two validation datasets. The bottom left is the trained LSTM emulation and the bottom right is the original output from the CESM2. CESM2 model data is only available until 2014, so that year is used as a comparison. The darker grid cells indicate more carbon stored in AGB.

Ecozone	Matasci et al. (Mt C)	Walker et al. (Mt C)	ERANFIS (Mt C)	CESM2 (M
Boreal Shield	8837.93	5294.87	6998.04	9329.47
Boreal Cordillera	1578.7	906.74	2920.79	2547.19
Boreal Plain	4165.49	2092.03	2947.92	4647.0
Total	14582.13	8293.64	12866.74	16523.66

TABLE 3.5: Total AGB carbon comparisons for Matasci et al, Walker et al., ERANFIS and the original output from the CESM2. All values are in Mt C. Total is the sum of all three ecozones.

It is important to note that Sothe et al. find significant carbon stocks in the Hudson Plains, an ecozone that contains the majority of Canada's wetlands (Sothe et al., 2022). Neither the CESM2 nor the emulation simulate a significant amount of carbon to this region. As for AGB, the emulation estimates values that are very similar across ecozones, with the smallest amount of variation between the ecozones.

3.4.1 Explainability

I used two feature attribution methods to help explain the model's output and improve confidence in the model's predictions. Explainability methods help to provide explanations of models behaviours after inference. These methods are not meant to

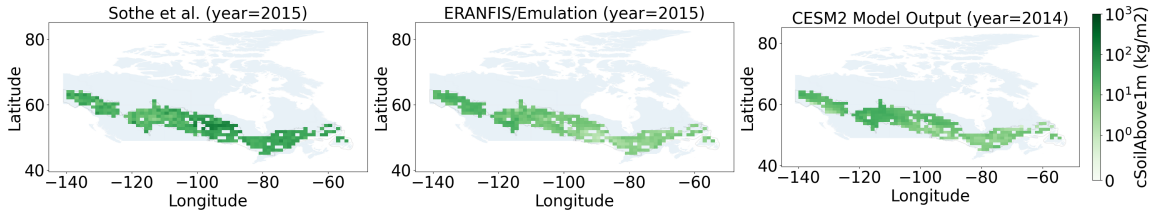

FIGURE 3.6: Spatial visualization of soil carbon comparison. Note the significantly larger quantities for Sothe. et al. The Hudson Plains was found to be a large soil carbon store.

Model	R^2	**Average LAMSE (kg/m^2)**
Sothe et al.		
ERANFIS	-1.02	1405.37
CESM2	-1.00	1396.12

TABLE 3.6: Evaluation metrics for ERANFIS and CESM2 compared to Sothe et al. Both models differ significantly from Sothe et al.

Ecozone	**Sothe et al. (Mt C)**	**ERANFIS (Mt C)**	**CESM2 Model Output (Mt C)**
Boreal Shield	67565.9	8832.3	12931.02
Boreal Cordillera	10047.73	7073.49	5172.8
Boreal Plain	16702.99	8162.71	13199.31
Total	94316.62	24068.51	31303.14

TABLE 3.7: Total soil carbon comparisons for Sothe et al., ERANFIS and the CESM2. The total is the sum of all three ecozones. All values are in Mt C.

replace the physical laws that process-based climate models are built on, but instead to improve confidence that the ML model is learning in the right direction. Integrated Gradients (IG), which determines the importance of features by taking the integral of the ML model's gradients along a straight path from a baseline (a zero vector, which in this case is the mean of the normalized data) to the input, and Shapley values, which are used to help understand a feature's contribution to the output (Sundararajan et al. (2017), Lundberg and Lee (2017)). Here I used IG for cStem (the largest contributor to AGB) and I used ERANFIS to understand the predictions of the model. To do so, I took the mean of the attributions for a single grid cell (see Figure 7). Correlations between physical processes and results from emulations help to increase confidence in machine learning models and can help explain the results of the model (Holzinger et al., 2022).

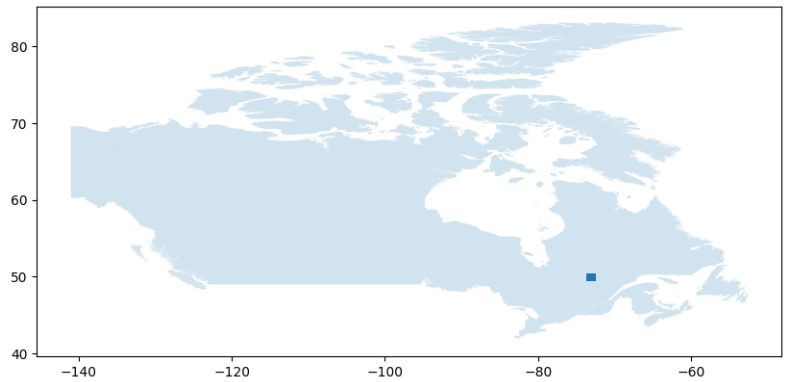

FIGURE 3.7: Grid cell (longitude=-73.75, latitude = 49.476440) used for explainability techniques. This a region in the eastern Boreal Shield.

In Figure 8 and Figure 9 we can see the feature attributions for the cStem variable. The cStem variable is the most significant contributor to AGB and provides the strongest signal for feature attribution (see Supplemental Materials). The mean of ERANFIS for each variable is in the center of the y axis for each variable to aid visualization. The attribution spans the 30-year window from 1985-2014. We can see in Figure 8 that the higher values of tsl and tas_{JJA} (i.e. hot soil and summer temperatures) negatively contribute to cStem. Low values of pr also contribute negatively to cStem. Figure 9 shows that higher values of precipitation and above-average treeFrac values positively contribute to the cStem variable. Scientifically this makes sense - warmer soil temperatures have been found to hold less carbon (similarly for precipitation, Hartley et al. (2021)).

I applied the Shapley value solution and find that the results generally echo the findings of IG although there are some differences (see Figures 10 and 11). The Shapley values clearly indicate that higher soil temperature (tsl) leads to higher positive impact on the model, whereas the Integrated Gradients method shows no strong signal for the soil temperature. The Shapley values were averaged across the three AGB target variables and the soil target variable separately for each grid cell. We can see that for both soil and AGB target variables they have similar results. High values of tree cover seldom negatively attribute, although the impacts are very noisy. Other vegetation has been found to hold more soil carbon (shrubs and grass) and could explain how grid cells with lower treeFrac contribute positively to the target variables (Canadell et al., 2021).

3.4.2 Wood Harvest Scenario

The benefit of creating an emulation of a climate model is to be able to explore climatic scenarios that would otherwise require significant computational resources. In this spirit, I created two scenarios to understand the impacts of wood harvest on carbon stocks. Because of the significant discrepancy of observed and modeled soil

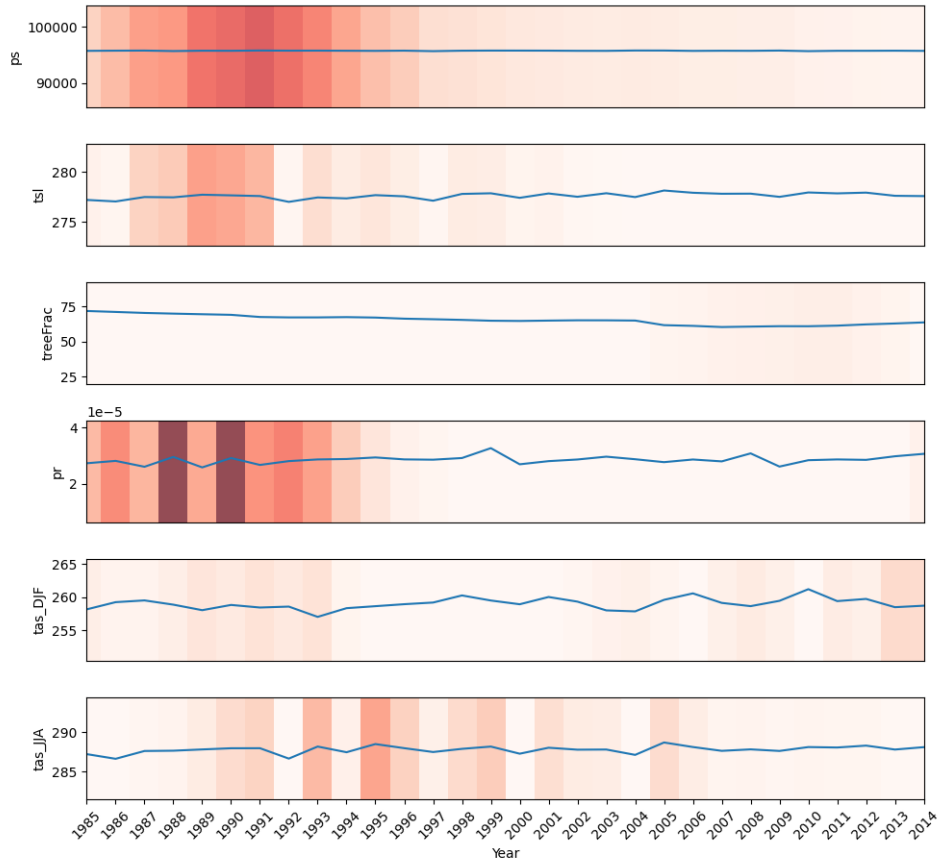

FIGURE 3.8: Negative Attributions for cStem. The darker colour represents higher attribution, a stronger negative contribution to the output of the model. The y-axis is centered on the mean of the entire input dataset, with two standard deviations above and below. Each vertical bar in the plots represents a year.

carbon stocks, the soil carbon stock results in these scenarios should be interpreted with caution. For comparison to other studies, the soil carbon results are omitted.

I created two scenarios from an additional land-cover product that quantifies wood harvest for the years 1985-2019 (Hermosilla et al., 2016). The first scenario assumes all wood harvest for the years 1985-2019 is replaced by forested area. This scenario can be thought of as an alternate reality where the wood harvest did not occur for the years 1985-2019. This was done by adding the percentage of area harvested per grid cell to the treeFrac variable in ERANFIS. In all other respects the input data is the same as ERANFIS. By simulating reforestation of areas deforested from wood harvest, the simulation adheres to ensuring food security and biodiversity remain intact, assuming the harvested land was not converted to cropland.

I created a second scenario that assumes that wood harvest occurred but without

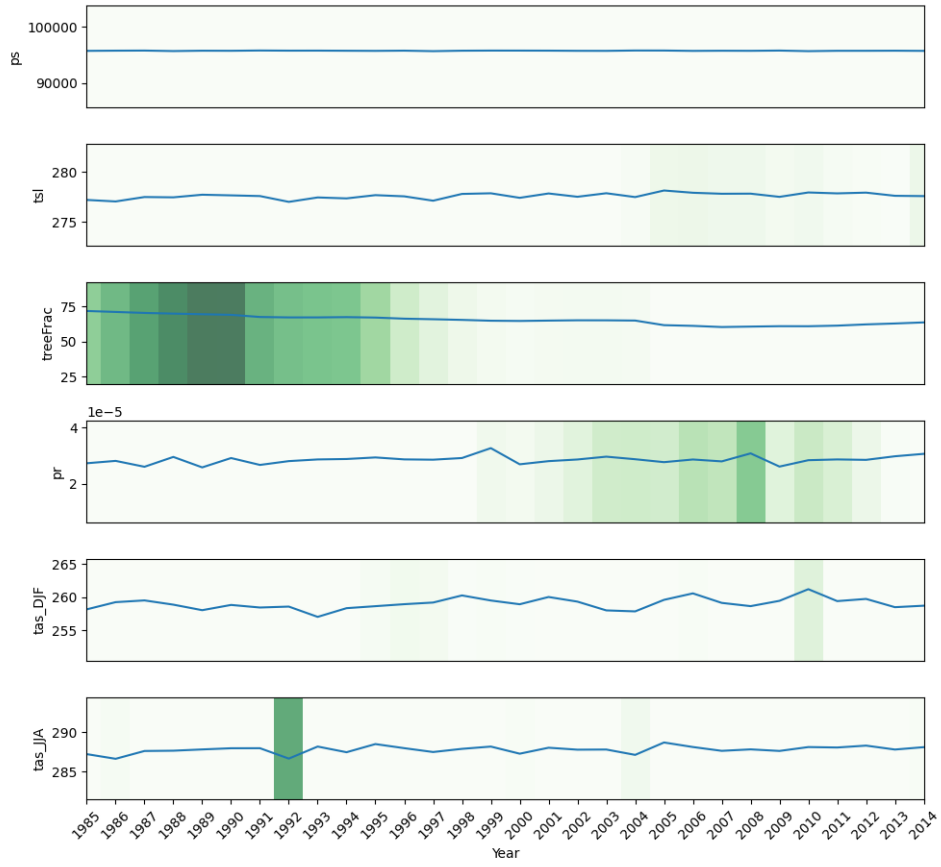

FIGURE 3.9: Positive Attributions for cStem. The darker colour represents higher attribution, a stronger positive contribution to the output of the model. The y-axis is centered on the mean of the entire input dataset, with two standard deviations above and below. Each vertical bar in the plots represents a year.

any subsequent regrowth. This scenario is made by finding all the areas that were harvested in the study period and subsequently were classified as tree-covered.

I applied the emulation to the reforested scenario and to the no regrowth scenario. I then took the difference of carbon stocks and quantified this as carbon lost due to wood harvest. Because of the 30-year time series used in the experiment, only the years 2014-2019 are used for analysis. When the reforested scenario is compared with ERANFIS, 412 Mt C is sequestered in above-ground biomass and 516 Mt C is sequestered in soil carbon by the year 2019 using the reforestation scenario. When the no regrowth scenario is compared to ERANFIS, 172 Mt C in AGB and 88 Mt C in soil carbon is attributed to regrowth (see Figure 12). In total, 584 Mt C of AGB and 604 Mt of soil carbon is lost to wood harvest over the study period, although 172 Mt C and 88 Mt C respectively has grown back. The 584 Mt of AGB carbon accounts for

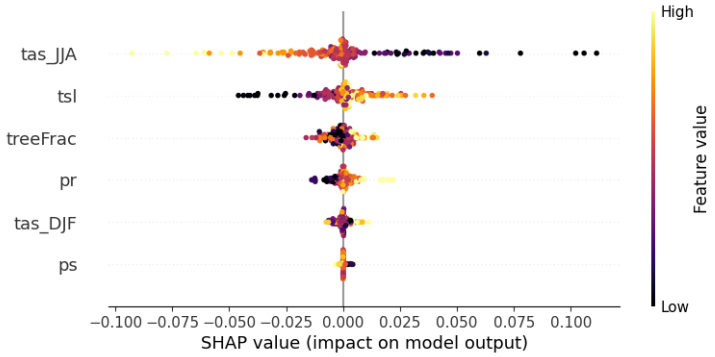

FIGURE 3.10: Shapley values for AGB target variables. The yellow colour indicates a higher value and the placement along the x-axis indicates the impact on model output. Values further to the right indicate higher positive impact.

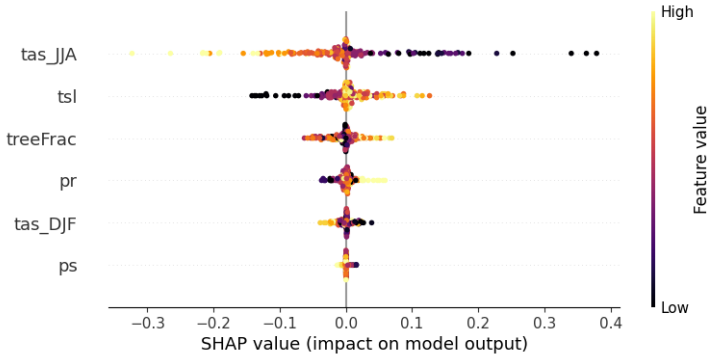

FIGURE 3.11: Shapley values for the soil target variable. The yellow colour indicates a higher value and the placement along the x-axis indicates the impact on model output. Values further to the right indicate higher positive impact.

approximately 1.5% of the total estimated AGB carbon in the study area. Overall, reforestation leads to 1188 Mt C gained over the study period.

In general, Figures 14 and 15 show an increase of carbon storage in both AGB carbon and soil carbon where there is more forest cover. Both figures show there are grid cells that have more soil carbon in no-regrowth scenarios and more soil carbon in ERANFIS instead of the reforested scenario. As the CESM2 represents agricultural management and land-use change, the increase in soil carbon on these grid cells could be attributed to increased soil carbon storage of grasslands and crops when compared to tree cover (Canadell et al. (2021),Lawrence et al. (2019), David Lawrence et al. (2018)).

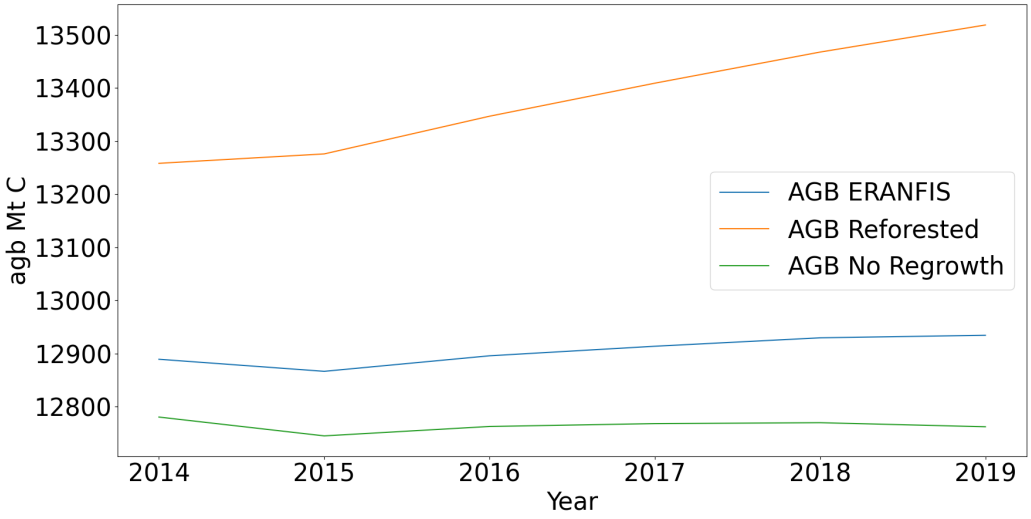

FIGURE 3.12: Yearly comparison for harvest scenarios. Each year represents the total AGB carbon for the study area.

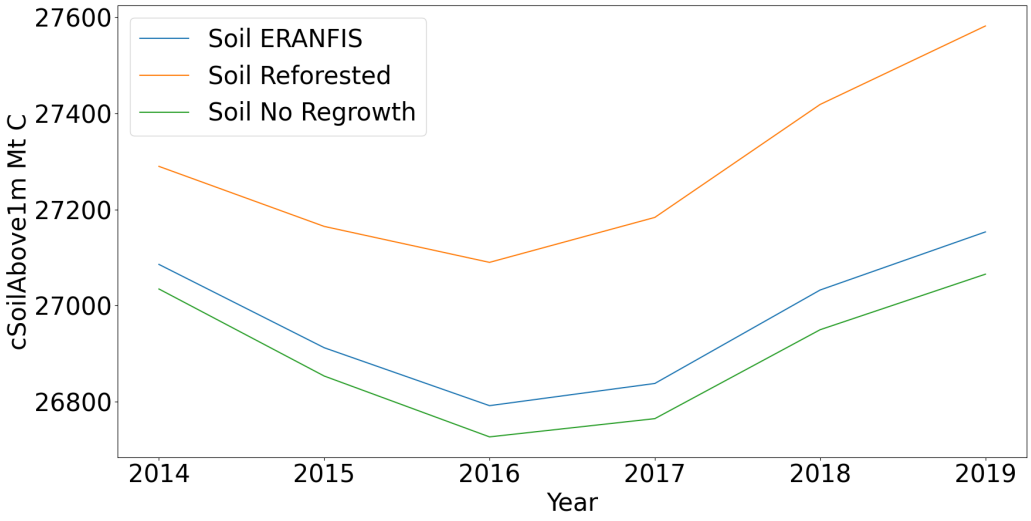

FIGURE 3.13: Yearly comparison for harvest scenarios. Each year represents the total soil carbon for the study area.

3.5 Discussion

A significant portion of Canada's emissions reported in the National Inventory Report (NIR) is attributed to land-use and land cover change (LULCC) (Canada, 2023). Harvested Wood Products (HWP) is all wooded material that leaves harvest sites in

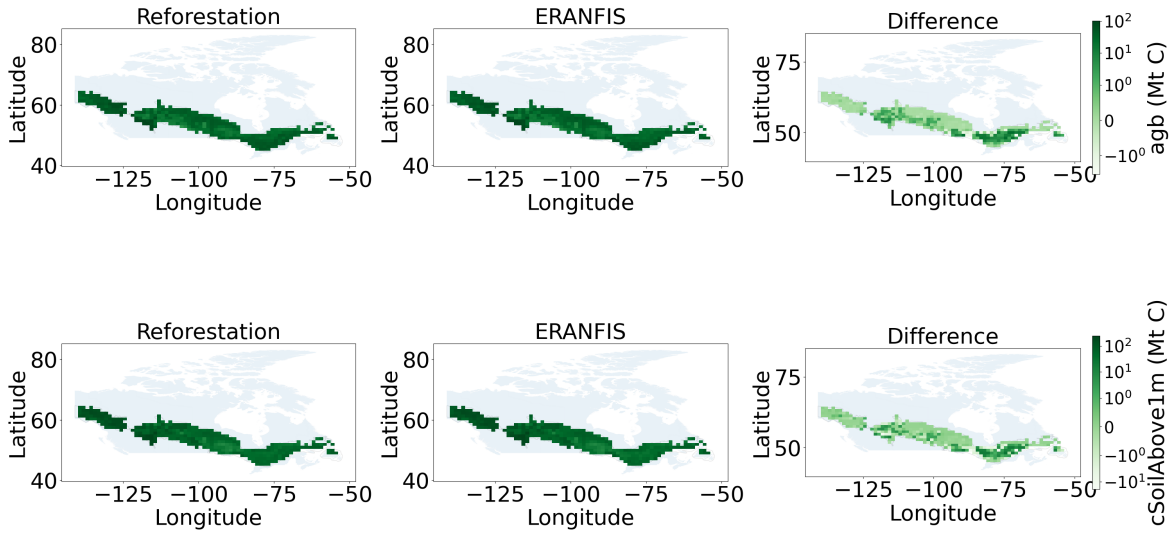

FIGURE 3.14: Scenario that sees all previously harvested forest reforested. From left to right: The reforested estimations, the emulated estimations and the difference between the two scenarios. Note the difference in scale between the images.

AGB			
Ecozone	**Reforested Scenario (Mt C)**	**No-regrowth Scenario (Mt C)**	**ERANFIS (M**
Boreal Shield	7523.80	6904.01	7046.49
Boreal Cordillera	2962.24	2954.80	2955.64
Boreal Plain	3032.18	2903.64	2932.39
Total	13518.22	12762.46	12934.52
Soil			
Boreal Shield	10973.56	10563.48	10634.74
Boreal Cordillera	8083.69	8071.37	8072.21
Boreal Plain	8524.70	8430.31	8446.18
Total	27581.97	27065.17	27153.14

TABLE 3.8: Total carbon (Mt C) in 2019 for the reforest scenario and the no-regrowth scenario for both AGB and soil carbon.

the IPCC Guidelines for National Greenhouse Gas Inventories and plays an important part in Canada's GHG reporting (H Eggleston et al., 2006). HWP is a carbon pool that holds all the carbon captured by wood transferred from harvest (H Eggleston et al., 2006). The wood harvest scenario used in this research can be considered an accounting method tracking carbon transfer from forest to the HWP pool. In the 2021 NIR, Canada reports this value as "Commercial harvest transfers to HWP"

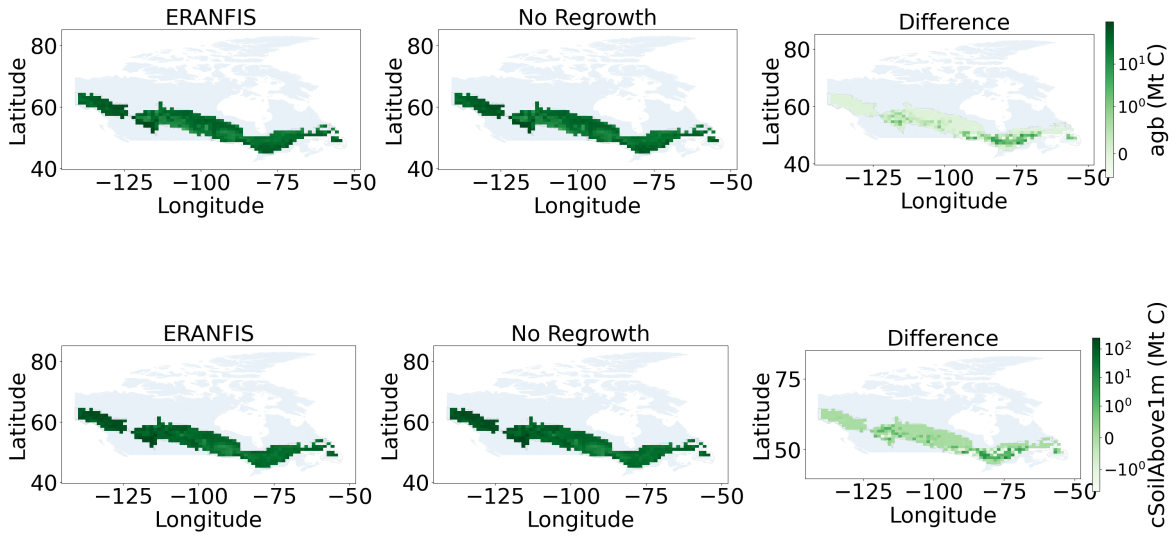

FIGURE 3.15: Scenario that sees all regrowth in harvested areas removed. From left to right: ERANFIS estimations, the no-regrowth estimations and the difference between the two. In this case it is (Observed - No-regrowth) as the no-regrowth will have smaller values.

(Canada, 2023). The report finds that approximately 25 Mt C are transferred per year from the years 1990-2021 (Canada, 2023). In 2021, almost 30 Mt C was reported, equivalent to 109 Mt CO_2, a significant portion of Canada's 670 Mt CO_2 net emissions for 2021 (Canada, 2023). All of these emissions are offset by forest carbon sequestration and the sector reports a net sink, but looking at gross emissions caused by wood harvest better highlights the potential for carbon mitigation (Canada, 2023). This shows the importance of being able to accurately account for the impact of wood harvest on carbon stores as it has the potential to make a significant contribution to the reduction of GHG emissions nationally.

The quantities found in this paper are different than what is reported in the 2021 NIR - I found in this study that from 1984-2019, 584 Mt C of AGB carbon were attributed to wood harvest emissions. This amount averaged over the study period is 16.7 Mt C per year of carbon emissions. The study area is 52.2% of Canada's forested area (see Table 1) but accounts for more than half of the reported values in the NIR. The NIR uses the entire national forest cover, and considers total ecosystem carbon instead of only AGB considered here. The NIR uses the Carbon Budget Model of the Canadian Forest Sector (CBM-CFS3), a process-based climate model that focuses on forest dynamics and uses forest disturbance data from the National Forestry Database (Canada (2023),Kurz et al. (2013)).

Another study that uses the same land-cover products finds a significantly higher

loss of AGB due to wood harvest over the same period (Wulder et al., 2020). Wulder et al. reports for the three ecozones used in this study, at 800 Mt C lost due to wood harvest from the years 1985-2016 with an average loss of 25 Mt C per year. Wulder et al. use allometric equations combined with lidar and satellite imagery to quantify AGB dynamics Wulder et al. (2020). Pan et al. 2011 finds 23 Mt C carbon per year lost due to wood harvest from 1990-1999 and 21 Mt C per year lost from 2000-2009 for all of Canada. This is within the uncertainty range provided by Pan et al., although it is at the lowest end of this range (Pan et al., 2011). Pan et al. gather national inventory data and observational sources to make global forest carbon storage estimations (Pan et al., 2011).

The AGB carbon quantities I found in this study (16.7 Mt C per year) are within plausible range of values when compared to other studies. Wulder et al. overestimates AGB carbon (25 Mt C per year, same study area) compared to this study, and both the NIR (25 Mt C per year,total ecosystem carbon and for all of Canada) and Pan et al. (22 Mt C per year, all of Canada) underestimate forest carbon in comparison (Pan et al. (2011),Wulder et al. (2020),Canada (2023)).

The IPCC encourages consideration of differences in methods to understand better net emissions from land sectors (Joeri Rogelj et al., 2022). There is significant difference in method between the studies mentioned, and attributing quantities to the differences in the modelling approaches is not realistic, although it is encouraging that the approaches discussed here approximate similar quantities given different methodologies. There are many disparate methods to accounting for land carbon and comparison is integral to making a meaningful contribution.

Not only can reforestation or reduced wood harvest contribute to reducing GHG emissions, these practices can also reduce land degradation, preserve regional biodiversity and ensure other ecosystem services such as water filtration (Canadell et al., 2021). Forest management practices can have adverse side effects. By allocating land for forest, land meant for agriculture could be jeopardized. Forest management practices that reduce the forest species complexity can leave the forest vulnerable to natural disasters, such as invasive insect species that target a particular species of tree (Canadell et al., 2021). These factors, among others, need to be carefully considered when implementing forest management practices such as reforestation or afforestation.

The method used to replace harvested forest regions with tree cover neglects the impact of the additional tree cover on the other climatic variables (Mills et al., 2023). Recent research has found that idealized research such as the work done here leaves out important climatic signals of forest cover change (Alkama and Cescatti, 2016). Changes in forest cover can have a significant impact on surface air temperature and surface albedo which is not considered in the wood harvest scenario, as the tree-cover fraction is changed without considering the effect of this change on the other input variables (Alkama and Cescatti (2016) Mills et al. (2023)). Harvested areas can lead to greater above-ground biomass gain, but recently it has been found that the loss of soil carbon can eclipse this gain, and can be considered a carbon

source (Mills et al., 2023). Climate model emulations are at the mercy of the scientific choices made in the process-based models being emulated; machine learning emulations are not able to account for changing physical processes, although effort is being made to change this by incorporating physical laws into machine learning models, a technique often called "physics-informed machine learning" (Karniadakis et al., 2021). These methods could help confidence in climate model emulations by providing a physical basis on which estimations are made.

To help explain estimations made in this study two techniques were used. These techniques, IG and Shapley values, assess the importance of each feature to the output. While these techniques cannot be taken as surrogates for physical processes, it can guide understanding of the model's behaviour and output. More recent efforts have incorporated scenarios that test an emulator's ability to respond accurately to the change in input (Watson-Parris et al., 2022). For example, Watson-Parris et al., when using an emulation trained to predict atmospheric temperature, create an experiment where only aeresol forcings are used (Watson-Parris et al., 2022). This more nuanced testing can help increase confidence by rooting the experimentation in well-known physical processes. It is difficult to assess the impact of omitting these feedbacks on emulation, but through further comparison progress can be made to increase confidence that emulations are providing accurate and holistic predictions. This research only considers two aspects of forest carbon (soil carbon to 1m depth, and carbon in above-ground biomass) for reasons of comparability, as the literature often isolates AGB and soil carbon to 1m depth ((Sothe et al., 2022), see Results).

3.5.1 Further Work

Creating more nuanced scenarios, perhaps with other land-cover scenario efforts (e.g. https://luh.umd.edu/) could be a fruitful avenue of research. These scenarios could take into account regrowth dynamics and effects that forest cover has on climatic variables. The wood-harvest scenarios created in this study do not define what is replacing the tree cover that has been harvested. Considering the variation that different land-cover classes have on carbon stocks, this is a significant factor to exclude. A more nuanced wood harvest scenario could be made with explicit land-use change taking place.

Exploring different model architectures could improve performance and interpretability. Architectures exist that considers both spatial and temporal dimensions, which could be applied to climate model output. Exploring different rolling-window sizes, feature selections and model inputs could also improve model performance. Recent efforts using variations of the transformer model architecture have proven effective at learning climate and weather tasks, and could improve estimations in this domain (Nguyen et al., 2023) (Bi et al., 2022). As both machine learning techniques and process-based understanding of forest dynamics improve, we will better be able to predict and estimate carbon stocks and anthropogenic impacts on these stocks.

3.6 Conclusion

I used machine learning to emulate the CESM2, which I then used to estimate carbon stock loss due to wood harvest. I began by applying the emulation to ERANFIS (a dataset created from ERA5 reanalysis data and NFIS land-cover classification to create a dataset that more closely resembles actual climate) and comparing this to CESM2 estimates of forest carbon. The estimates provided from ERANFIS are significantly different from CESM2 as the input datasets are substantially different. I then compared ERANFIS to several datasets based on remote-sensing observations. In this comparison, ERANFIS performs better than the CESM2 when compared to AGB datasets, although neither perform well against the soil carbon dataset. I then utilized a land-cover dataset that represents wood harvest to create two land-cover scenarios: one in which no wood harvest occurred, and one where wood harvest occurred with no subsequent regrowth. I took these land-cover scenarios and applied the machine-learning emulation to them, which produced estimations of AGB and soil carbon. The model estimates that for the period 1985-2019, 584 Mt C was lost due to wood harvest. This does not include the 172 Mt C attributed to regrowth for the same period. These values are within a reasonable range of several other attempts to quantify impacts of wood harvest, which can be used together to help inform climate mitigation policy and action. This research highlights the synergy between process-based climate models and machine learning. By employing an LSTM model to learn relationships of climatic processes employed by the CESM2, I was able to investigate novel land-use change scenarios forest carbon dynamics with significantly lower computational costs. Machine learning emulation will increase accessibility to powerful climate models that can provide important information to inform policy and help guide climate change mitigation. Here I have investigated net loss from carbon to illuminate both the climate impact of wood harvest alone, as well as the carbon mitigation potential of reforestation efforts.

3.7 Data availability

Please see github.com/grahamclyne/thesis

3.8 Conflicts of interest

The authors declare no conflict of interest.

3.9 Supplementary Material

Figures S1 and S2 outline a significant deficiency in the emulation - the model is not good at predicting outliers. In Figure S2, we can see that the values are less varied than the other models. When summed by ecozone in Table 5 and Table 7, the emulation indicates noticeably less variance than the observed datasets. We can see the standard deviations of the predictions in Figure S1 are smaller than the trained data. In the aggregate this model is able to accurately assess carbon stores, but for smaller regions it is unable to estimate large differences in carbon stores. By using multiple climate models as inputs, or by using a model architecture that has been shown to generalize better, such as a transformer, estimations for more extreme carbon stocks could be improved.

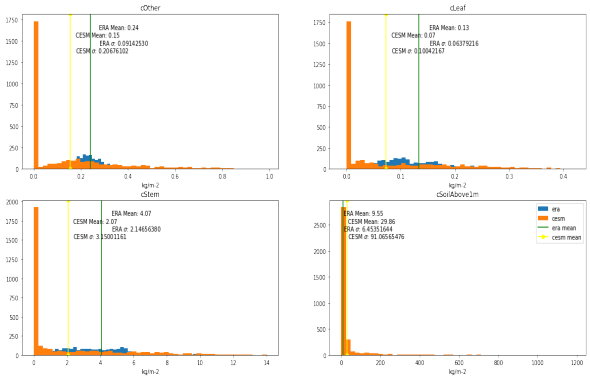

FIGURE 3.16: Distributions of the four target variables used in the LSTM model.

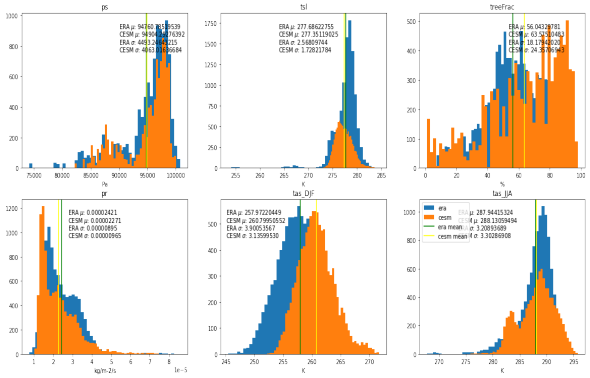

FIGURE 3.17: Distributions of the input variables used in the LSTM model.

Figures S3-S8 show the comparisons between each input variable for ERANFIS and CESM2.

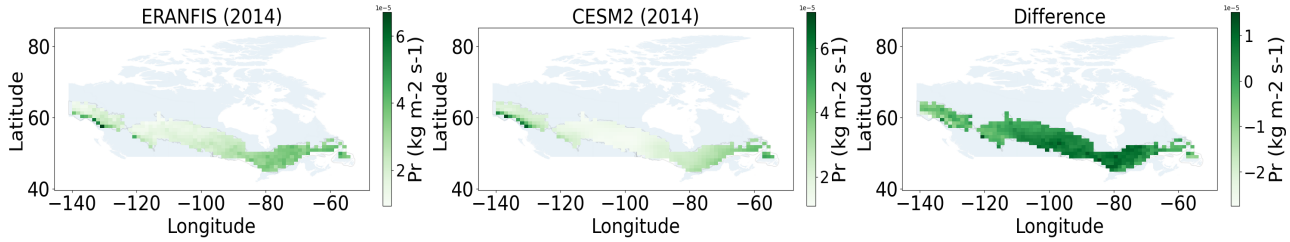

FIGURE 3.18: Comparison of precipitation.

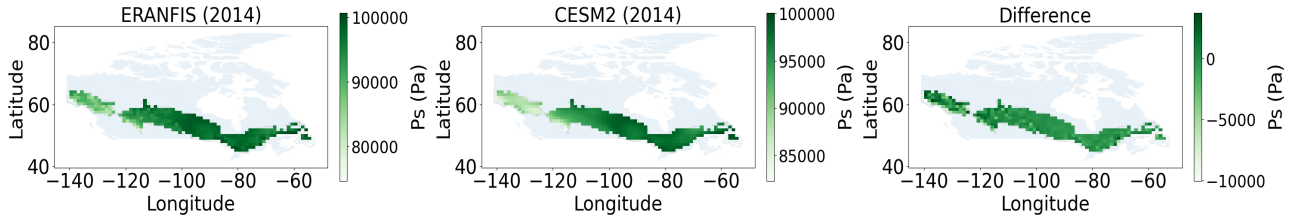

FIGURE 3.19: Comparison of surface pressure.

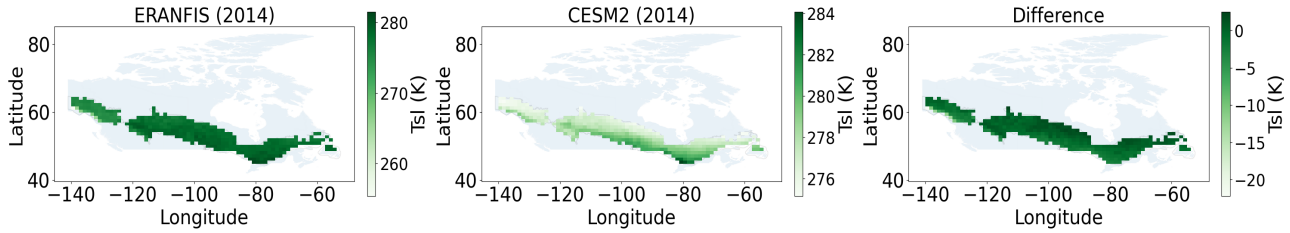

FIGURE 3.20: Comparison of soil temperature.

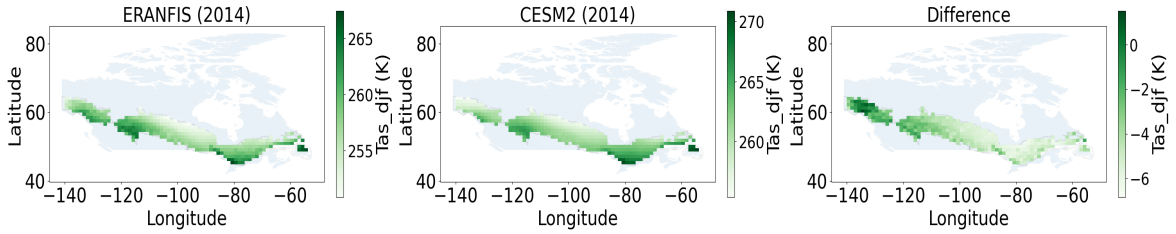

FIGURE 3.21: Comparison of surface air temperature for December,January and February.

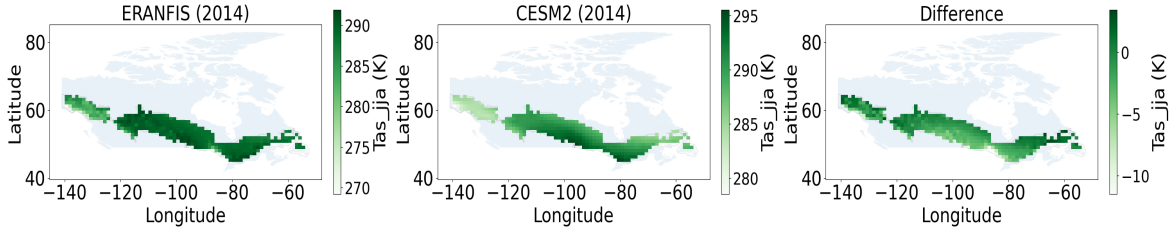

FIGURE 3.22: Comparison of surface air temperature for June,July and August.

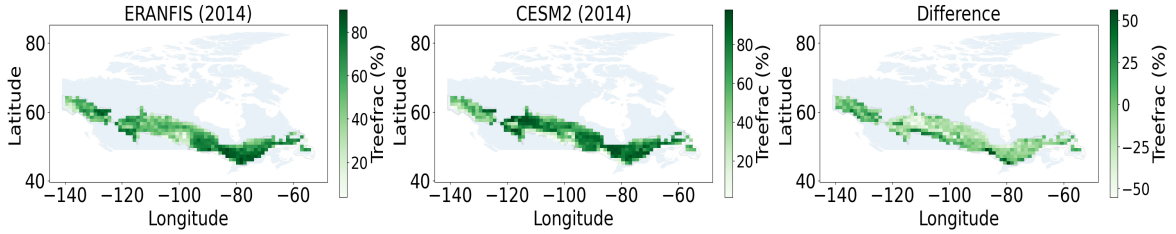

FIGURE 3.23: Comparison of tree fraction cover.

Chapter 4

Conclusion

This research helps to highlight the synergy between process-based climate models and machine learning. By employing an LSTM to learn relationships of climatic processes described by the CESM2, I was able to investigate difficult-to-observe forest carbon dynamics with significantly lower computational costs. Emulating climate models can be helpful in exploring scenarios with changing land-use and land cover dynamics when coupled with detailed land-cover classification products. I was able to understand the impacts of wood harvest in the Canadian Boreal forest by simulating several variables of the CESM2 with an LSTM model. This model performed well learning the dataset, obtaining an R^2 score of .89. I then created a dataset of climatic data based on ERA5 data and NTEMS land-cover data. I then applied the model emulation to this dataset to help understand the climate based on real-world observations, instead of climate model output simulated by a climate model. Comparing this data to several AGB observation-based datasets, I find that the ERA5/NTEMS dataset correlates more to the datasets than the CESM2 does, and provides a closer total carbon stock. When compared to an external soil carbon dataset, the emulation and the CESM2 perform comparably, although both estimate significantly lower soil carbon stocks mostly due to a large carbon store in the Hudson Plains indicated in the external dataset.

To help increase confidence in the model, I use two feature attribution methods, Integrated Gradients and Shapley values. In both cases, the feature attributions are concurrent with physical understandings of biogeophysical processes.

Finally, to answer the question, "What is the impact of wood harvest on Canadian Boreal forests?" I create two more datasets that represent two scenarios - one where no wood harvest occurred and another where no forest regrowth occurred in places of wood harvest. Using these two datasets, I again apply the emulation and find that 409 Mt C was sequestered by the year 2019 in the "no wood harvest" scenario. This is not including the 129 Mt C attributed to regrowth in the same region found in the "no regrowth from wood harvest" scenario. This 409 Mt C is equivalent to 1497 Mt CO_2. For the study period 1985-2019 this is 50 Mt CO_2 per year, a substantial contribution to Canada's net GHG emissions (670 Mt CO_2 in 2021). The contribution from LULCC in the 2021 NIR released by Canada is a carbon sink because of the large amount of carbon sequestration provided by the forest. Here I have investigated

net loss from carbon to illuminate both the climate impact of wood harvest alone, as well as the carbon mitigation potential of reforestation efforts.

Reforestation and reduction in wood harvest as a nature-based solution is a viable and effective method to mitigate climate change. Increasing forest cover can help sequester carbon and help achieve a more sustainable environment. Moreover, reducing wood harvest can help conserve existing forests and limit the amount of carbon released into the atmosphere through deforestation. While this should be complemented by other measures, it is an important step towards reducing GHG emissions.

Bibliography

R. Alkama and A. Cescatti. Biophysical climate impacts of recent changes in global forest cover. *Science*, 351(6273):600–604, Feb. 2016. ISSN 0036-8075, 1095-9203. doi: 10.1126/science.aac8083. URL https://www.science.org/doi/10.1126/science.aac8083.

W. R. Anderegg, A. T. Trugman, G. Badgley, C. M. Anderson, A. Bartuska, P. Ciais, D. Cullenward, C. B. Field, J. Freeman, S. J. Goetz, J. A. Hicke, D. Huntzinger, R. B. Jackson, J. Nickerson, S. Pacala, and J. T. Randerson. Climate-driven risks to the climate mitigation potential of forests. *Science*, 368(6497), 2020. ISSN 10959203. doi: 10.1126/science.aaz7005.

P. A. Arias, N. Bellouin, R. G. Jones, V. Naik, G.-K. Plattner, J. Rogelj, J. Sillmann, T. Storelvmo, P. W. Thorne, B. Trewin, K. A. Rao, B. Adhikary, R. P. Allan, K. Armour, R. Barimalala, J. G. Canadell, C. Cassou, A. Cherchi, W. Collins, S. Corti, F. Cruz, F. J. Dentener, C. Dereczynski, A. D. Luca, A. Diongue, F. J. Doblas-Reyes, A. Dosio, H. Douville, F. Engelbrecht, J. C. Fyfe, N. P. Gillett, and L. Goldfarb. Technical Summary. *Climate Change 2021: The Physical Science Basis. Contribution of Working Group I to the Sixth Assessment Report of the Intergovernmental Panel on Climate Change*, 2021.

K. Bi, L. Xie, H. Zhang, X. Chen, X. Gu, and Q. Tian. Pangu-Weather: A 3D High-Resolution Model for Fast and Accurate Global Weather Forecast, Nov. 2022. URL http://arxiv.org/abs/2211.02556. arXiv:2211.02556 [physics].

Canada, editor. *National inventory report: greenhouse gas sources and sinks in Canada: executive summary*. Environment Canada, Ottawa, 2023. ISSN: 2371-1329 Medium: electronic resource.

J. G. Canadell, P. M. Monteiro, M. H. Costa, S. Syampungani, S. Zaehle, K. Zickfeld Canada, and G. A. Alexandrov. *2021: Global Carbon and other Biogeochemical Cycles and Feedbacks. In Climate Change 2021: The Physical Science Basis. Contribution of Working Group I to the Sixth Assessment Report of the Intergovernmental Panel on Climate Change*. 2021. ISBN 978-1-00-915789-6. doi: 10.1017/9781009157896.007.674. Publication Title: Ipcc.

R. L. Chazdon, P. H. Brancalion, L. Laestadius, A. Bennett-Curry, K. Buckingham, C. Kumar, J. Moll-Rocek, I. C. G. Vieira, and S. J. Wilson. When is a forest a forest? Forest concepts and definitions in the era of forest and landscape restoration. *Ambio*, 45(5):538–550, 2016. ISSN 16547209. doi: 10.1007/s13280-016-0772-y.

K. Dagon, B. M. Sanderson, R. A. Fisher, and D. M. Lawrence. A machine learning approach to emulation and biophysical parameter estimation with the Community Land Model, version 5. *Advances in Statistical Climatology, Meteorology and Oceanography*, 6(2):223–244, Dec. 2020. ISSN 23643587. doi: 10.5194/ascmo-6-223-2020. Publisher: Copernicus GmbH.

G. Danabasoglu, J. F. Lamarque, J. Bacmeister, D. A. Bailey, A. K. DuVivier, J. Edwards, L. K. Emmons, J. Fasullo, R. Garcia, A. Gettelman, C. Hannay, M. M. Holland, W. G. Large, P. H. Lauritzen, D. M. Lawrence, J. T. Lenaerts, K. Lindsay, W. H. Lipscomb, M. J. Mills, R. Neale, K. W. Oleson, B. Otto-Bliesner, A. S. Phillips, W. Sacks, S. Tilmes, L. van Kampenhout, M. Vertenstein, A. Bertini, J. Dennis, C. Deser, C. Fischer, B. Fox-Kemper, J. E. Kay, D. Kinnison, P. J. Kushner, V. E. Larson, M. C. Long, S. Mickelson, J. K. Moore, E. Nienhouse, L. Polvani, P. J. Rasch, and W. G. Strand. The Community Earth System Model Version 2 (CESM2). *Journal of Advances in Modeling Earth Systems*, 12(2), Feb. 2020. ISSN 19422466. doi: 10.1029/2019MS001916. Publisher: Blackwell Publishing Ltd.

David Lawrence, Rosie Fisher, and Charles Koven. CLM5 Technical Note, 2018. URL https://www2.cesm.ucar.edu/models/cesm2/land/CLM50_Tech_Note.pdf.

D. A. DellaSala, H. Keith, T. Sheehan, J. Strittholt, B. Mackey, M. Connolly, J. R. Werner, and A. L. Fredeen. Estimating carbon stocks and stock changes in Interior Wetbelt forests of British Columbia, Canada. *Ecosphere*, 13(4):1–18, 2022. ISSN 21508925. doi: 10.1002/ecs2.4020.

A. Doury, S. Somot, S. Gadat, A. Ribes, and L. Corre. Regional climate model emulator based on deep learning: concept and first evaluation of a novel hybrid downscaling approach. *Climate Dynamics*, 2022. ISSN 14320894. doi: 10.1007/s00382-022-06343-9. Publisher: Springer Science and Business Media Deutschland GmbH.

P. Friedlingstein, M. O'Sullivan, M. W. Jones, R. M. Andrew, L. Gregor, J. Hauck, C. Le Quéré, I. T. Luijkx, A. Olsen, G. P. Peters, W. Peters, J. Pongratz, C. Schwingshackl, S. Sitch, J. G. Canadell, P. Ciais, R. B. Jackson, S. R. Alin, R. Alkama, A. Arneth, V. K. Arora, N. R. Bates, M. Becker, N. Bellouin, H. C. Bittig, L. Bopp, F. Chevallier, L. P. Chini, M. Cronin, W. Evans, S. Falk, R. A. Feely, T. Gasser, M. Gehlen, T. Gkritzalis, L. Gloege, G. Grassi, N. Gruber, Gürses, I. Harris, M. Hefner, R. A. Houghton, G. C. Hurtt, Y. Iida, T. Ilyina, A. K. Jain, A. Jersild, K. Kadono, E. Kato, D. Kennedy, K. Klein Goldewijk, J. Knauer, J. I. Korsbakken, P. Landschützer, N. Lefèvre, K. Lindsay, J. Liu, Z. Liu, G. Marland, N. Mayot, M. J. McGrath, N. Metzl, N. M. Monacci, D. R. Munro, S.-I. Nakaoka, Y. Niwa, K. O'Brien, T. Ono, P. I. Palmer, N. Pan, D. Pierrot, K. Pocock, B. Poulter, L. Resplandy, E. Robertson, C. Rödenbeck, C. Rodriguez, T. M. Rosan, J. Schwinger, R. Séférian, J. D. Shutler, I. Skjelvan, T. Steinhoff, Q. Sun, A. J. Sutton,

C. Sweeney, S. Takao, T. Tanhua, P. P. Tans, X. Tian, H. Tian, B. Tilbrook, H. Tsujino, F. Tubiello, G. R. van der Werf, A. P. Walker, R. Wanninkhof, C. Whitehead, A. Willstrand Wranne, R. Wright, W. Yuan, C. Yue, X. Yue, S. Zaehle, J. Zeng, and B. Zheng. Global Carbon Budget 2022. *Earth System Science Data*, 14(11): 4811–4900, Nov. 2022. ISSN 18663516. doi: 10.5194/essd-14-4811-2022. Publisher: Copernicus GmbH.

P. B. Gibson, W. E. Chapman, A. Altinok, L. Delle Monache, M. J. DeFlorio, and D. E. Waliser. Training machine learning models on climate model output yields skillful interpretable seasonal precipitation forecasts. *Communications Earth & Environment*, 2(1), 2021. ISSN 2662-4435. doi: 10.1038/s43247-021-00225-4. URL http://dx.doi.org/10.1038/s43247-021-00225-4. Publisher: Springer US.

F. Granata and F. Di Nunno. Forecasting evapotranspiration in different climates using ensembles of recurrent neural networks. *Agricultural Water Management*, 255, Sept. 2021. ISSN 18732283. doi: 10.1016/j.agwat.2021.107040. Publisher: Elsevier B.V.

B. W. Griscom, J. Adams, P. W. Ellis, R. A. Houghton, G. Lomax, D. A. Miteva, W. H. Schlesinger, D. Shoch, J. V. Siikamäki, P. Smith, P. Woodbury, C. Zganjar, A. Blackman, J. Campari, R. T. Conant, C. Delgado, P. Elias, T. Gopalakrishna, M. R. Hamsik, M. Herrero, J. Kiesecker, E. Landis, L. Laestadius, S. M. Leavitt, S. Minnemeyer, S. Polasky, P. Potapov, F. E. Putz, J. Sanderman, M. Silvius, E. Wollenberg, and J. Fargione. Natural climate solutions. *Proceedings of the National Academy of Sciences of the United States of America*, 114(44):11645–11650, 2017. ISSN 10916490. doi: 10.1073/pnas.1710465114.

H Eggleston, K. Tanabe, and S. Buendia. 2006 IPCC Guidelines for National Greenhouse Gas Inventories, July 2006.

Y. G. Ham, J. H. Kim, and J. J. Luo. Deep learning for multi-year ENSO forecasts. *Nature*, 573(7775):568–572, 2019. ISSN 14764687. doi: 10.1038/s41586-019-1559-7. URL http://dx.doi.org/10.1038/s41586-019-1559-7. Publisher: Springer US.

P. C. Hanson, A. B. Stillman, X. Jia, A. Karpatne, H. A. Dugan, C. C. Carey, J. Stachelek, N. K. Ward, Y. Zhang, J. S. Read, and V. Kumar. Predicting lake surface water phosphorus dynamics using process-guided machine learning. *Ecological Modelling*, 430:109136, 2020. ISSN 03043800. doi: 10.1016/j.ecolmodel.2020.109136. URL https://doi.org/10.1016/j.ecolmodel.2020.109136. Publisher: Elsevier B.V.

I. P. Hartley, T. C. Hill, S. E. Chadburn, and G. Hugelius. Temperature effects on carbon storage are controlled by soil stabilisation capacities. *Nature Communications*, 12(1), Dec. 2021. ISSN 20411723. doi: 10.1038/s41467-021-27101-1. Publisher: Nature Research.

T. Hermosilla, M. A. Wulder, J. C. White, N. C. Coops, G. W. Hobart, and L. B. Campbell. Mass data processing of time series Landsat imagery: pixels to data products for forest monitoring. *International Journal of Digital Earth*, 9(11):1035–1054, 2016. ISSN 17538955. doi: 10.1080/17538947.2016.1187673. URL https://doi.org/10.1080/17538947.2016.1187673. Publisher: Taylor & Francis.

T. Hermosilla, M. A. Wulder, J. C. White, N. C. Coops, and G. W. Hobart. Disturbance-Informed Annual Land Cover Classification Maps of Canada's Forested Ecosystems for a 29-Year Landsat Time Series. *Canadian Journal of Remote Sensing*, 44(1):67–87, Jan. 2018. ISSN 17127971. doi: 10.1080/07038992.2018.1437719. Publisher: Taylor and Francis Inc.

A. Holzinger, R. Goebel, R. Fong, T. Moon, K.-R. Müller, and W. Samek, editors. *xxAI - Beyond Explainable AI: International Workshop, Held in Conjunction with ICML 2020, July 18, 2020, Vienna, Austria, Revised and Extended Papers*, volume 13200 of *Lecture Notes in Computer Science*. Springer International Publishing, Cham, 2022. ISBN 978-3-031-04082-5 978-3-031-04083-2. doi: 10.1007/978-3-031-04083-2. URL https://link.springer.com/10.1007/978-3-031-04083-2.

D. N. Huntzinger, A. M. Michalak, C. Schwalm, P. Ciais, A. W. King, Y. Fang, K. Schaefer, Y. Wei, R. B. Cook, J. B. Fisher, D. Hayes, M. Huang, A. Ito, A. K. Jain, H. Lei, C. Lu, F. Maignan, J. Mao, N. Parazoo, S. Peng, B. Poulter, D. Ricciuto, X. Shi, H. Tian, W. Wang, N. Zeng, and F. Zhao. Uncertainty in the response of terrestrial carbon sink to environmental drivers undermines carbon-climate feedback predictions. *Scientific Reports*, 7(1):1–8, 2017. ISSN 20452322. doi: 10.1038/s41598-017-03818-2.

Joeri Rogelj, Drew Shindell, and Kejun Jiang. *Global Warming of 1.5°C: IPCC Special Report on Impacts of Global Warming of 1.5°C above Pre-industrial Levels in Context of Strengthening Response to Climate Change, Sustainable Development, and Efforts to Eradicate Poverty*. Cambridge University Press, 1 edition, June 2022. ISBN 978-1-00-915794-0 978-1-00-915795-7. doi: 10.1017/9781009157940. URL https://www.cambridge.org/core/product/identifier/9781009157940/type/book.

K. Johnson, F. N. Scatena, and Y. Pan. Short- and long-term responses of total soil organic carbon to harvesting in a northern hardwood forest. *Forest Ecology and Management*, 259(7):1262–1267, Mar. 2010. ISSN 03781127. doi: 10.1016/j.foreco.2009.06.049. Publisher: Elsevier.

G. E. Karniadakis, I. G. Kevrekidis, L. Lu, P. Perdikaris, S. Wang, and L. Yang. Physics-informed machine learning. *Nature Reviews Physics*, 3(6):422–440, June 2021. ISSN 2522-5820. doi: 10.1038/s42254-021-00314-5. URL https://www.nature.com/articles/s42254-021-00314-5. Number: 6 Publisher: Nature Publishing Group.

W. Kurz, C. Dymond, T. White, G. Stinson, C. Shaw, G. Rampley, C. Smyth, B. Simpson, E. Neilson, J. Trofymow, J. Metsaranta, and M. Apps. CBM-CFS3: A model of carbon-dynamics in forestry and land-use change implementing IPCC standards. *Ecological Modelling*, 220(4):480–504, Feb. 2009. ISSN 03043800. doi: 10.1016/j.ecolmodel.2008.10.018. URL https://linkinghub.elsevier.com/retrieve/pii/S0304380008005012.

W. Kurz, C. Shaw, C. Boisvenue, G. Stinson, J. Metsaranta, D. Leckie, A. Dyk, C. Smyth, and E. Neilson. Carbon in Canada's boreal forest — A synthesis. *Environmental Reviews*, 21(4):260–292, Dec. 2013. ISSN 1181-8700, 1208-6053. doi: 10.1139/er-2013-0041. URL http://www.nrcresearchpress.com/doi/10.1139/er-2013-0041.

W. A. Kurz, S. Hayne, M. Fellows, J. D. Macdonald, J. M. Metsaranta, M. Hafer, and D. Blain. Quantifying the impacts of human activities on reported greenhouse gas emissions and removals in Canada's managed forest: Conceptual framework and implementation. *Canadian Journal of Forest Research*, 48(10):1227–1240, 2018. ISSN 12086037. doi: 10.1139/cjfr-2018-0176. Publisher: Canadian Science Publishing.

R. Lam, A. Sanchez-Gonzalez, M. Willson, P. Wirnsberger, M. Fortunato, A. Pritzel, S. Ravuri, T. Ewalds, F. Alet, Z. Eaton-Rosen, W. Hu, A. Merose, S. Hoyer, G. Holland, J. Stott, O. Vinyals, S. Mohamed, and P. Battaglia. GraphCast: Learning skillful medium-range global weather forecasting. Dec. 2022. URL http://arxiv.org/abs/2212.12794. arXiv: 2212.12794.

D. M. Lawrence, R. A. Fisher, C. D. Koven, K. W. Oleson, S. C. Swenson, G. Bonan, N. Collier, B. Ghimire, L. van Kampenhout, D. Kennedy, E. Kluzek, P. J. Lawrence, F. Li, H. Li, D. Lombardozzi, W. J. Riley, W. J. Sacks, M. Shi, M. Vertenstein, W. R. Wieder, C. Xu, A. A. Ali, A. M. Badger, G. Bisht, M. van den Broeke, M. A. Brunke, S. P. Burns, J. Buzan, M. Clark, A. Craig, K. Dahlin, B. Drewniak, J. B. Fisher, M. Flanner, A. M. Fox, P. Gentine, F. Hoffman, G. Keppel-Aleks, R. Knox, S. Kumar, J. Lenaerts, L. R. Leung, W. H. Lipscomb, Y. Lu, A. Pandey, J. D. Pelletier, J. Perket, J. T. Randerson, D. M. Ricciuto, B. M. Sanderson, A. Slater, Z. M. Subin, J. Tang, R. Q. Thomas, M. Val Martin, and X. Zeng. The Community Land Model Version 5: Description of New Features, Benchmarking, and Impact of Forcing Uncertainty. *Journal of Advances in Modeling Earth Systems*, 11(12):4245–4287, Dec. 2019. ISSN 19422466. doi: 10.1029/2018MS001583. Publisher: Blackwell Publishing Ltd.

J. J. Lembrechts, J. van den Hoogen, J. Aalto, M. B. Ashcroft, P. De Frenne, J. Kemppinen, M. Kopecký, M. Luoto, I. M. Maclean, T. W. Crowther, J. J. Bailey, S. Haesen, D. H. Klinges, P. Niittynen, B. R. Scheffers, K. Van Meerbeek, P. Aartsma, O. Abdalaze, M. Abedi, R. Aerts, N. Ahmadian, A. Ahrends, J. M. Alatalo, J. M. Alexander, C. N. Allonsius, J. Altman, C. Ammann, C. Andres, C. Andrews, J. Ardö, N. Arriga, A. Arzac, V. Aschero, R. L. Assis, J. J. Assmann, M. Y. Bader,

K. Bahalkeh, P. Barančok, I. C. Barrio, A. Barros, M. Barthel, E. W. Basham, M. Bauters, M. Bazzichetto, L. B. Marchesini, M. C. Bell, J. C. Benavides, J. L. Benito Alonso, B. J. Berauer, J. W. Bjerke, R. G. Björk, M. P. Björkman, K. Björnsdóttir, B. Blonder, P. Boeckx, J. Boike, S. Bokhorst, B. N. Brum, J. Brůna, N. Buchmann, P. Buysse, J. L. Camargo, O. C. Campoe, O. Candan, R. Canessa, N. Cannone, M. Carbognani, J. Carnicer, A. Casanova-Katny, S. Cesarz, B. Chojnicki, P. Choler, S. L. Chown, E. F. Cifuentes, M. Čiliak, T. Contador, P. Convey, E. J. Cooper, E. Cremonese, S. R. Curasi, R. Curtis, M. Cutini, C. J. Dahlberg, G. N. Daskalova, M. A. de Pablo, S. Della Chiesa, J. Dengler, B. Deronde, P. Descombes, V. Di Cecco, M. Di Musciano, J. Dick, R. D. Dimarco, J. Dolezal, E. Dorrepaal, J. Dušek, N. Eisenhauer, L. Eklundh, T. E. Erickson, B. Erschbamer, W. Eugster, R. M. Ewers, D. A. Exton, N. Fanin, F. Fazlioglu, I. Feigenwinter, G. Fenu, O. Ferlian, M. R. Fernández Calzado, E. Fernández-Pascual, M. Finckh, R. F. Higgens, T. G. Forte, E. C. Freeman, E. R. Frei, E. Fuentes-Lillo, R. A. García, M. B. García, C. Géron, M. Gharun, D. Ghosn, K. Gigauri, A. Gobin, I. Goded, M. Goeckede, F. Gottschall, K. Goulding, S. Govaert, B. J. Graae, S. Greenwood, C. Greiser, A. Grelle, B. Guénard, M. Guglielmin, J. Guillemot, P. Haase, S. Haider, A. H. Halbritter, M. Hamid, A. Hammerle, A. Hampe, S. V. Haugum, L. Hederová, B. Heinesch, C. Helfter, D. Hepenstrick, M. Herberich, M. Herbst, L. Hermanutz, D. S. Hik, R. Hoffrén, J. Homeier, L. Hörtnagl, T. T. Høye, F. Hrbacek, K. Hylander, H. Iwata, M. A. Jackowicz-Korczynski, H. Jactel, J. Järveoja, S. Jastrzębowski, A. Jentsch, J. J. Jiménez, I. S. Jónsdóttir, T. Jucker, A. S. Jump, R. Juszczak, R. Kanka, V. Kašpar, G. Kazakis, J. Kelly, A. A. Khuroo, L. Klemedtsson, M. Klisz, N. Kljun, A. Knohl, J. Kobler, J. Kollár, M. M. Kotowska, B. Kovács, J. Kreyling, A. Lamprecht, S. I. Lang, C. Larson, K. Larson, K. Laska, G. le Maire, R. I. Leihy, L. Lens, B. Liljebladh, A. Lohila, J. Lorite, B. Loubet, J. Lynn, M. Macek, R. Mackenzie, E. Magliulo, R. Maier, F. Malfasi, F. Máliš, M. Man, G. Manca, A. Manco, T. Manise, P. Manolaki, F. Marciniak, R. Matula, A. C. Mazzolari, S. Medinets, V. Medinets, C. Meeussen, S. Merinero, R. d. C. G. Mesquita, K. Meusburger, F. J. Meysman, S. T. Michaletz, A. Milbau, D. Moiseev, P. Moiseev, A. Mondoni, R. Monfries, L. Montagnani, M. Moriana-Armendariz, U. Morra di Cella, M. Mörsdorf, J. R. Mosedale, L. Muffler, M. Muñoz-Rojas, J. A. Myers, I. H. Myers-Smith, L. Nagy, M. Nardino, I. Naujokaitis-Lewis, E. Newling, L. Nicklas, G. Niedrist, A. Niessner, M. B. Nilsson, S. Normand, M. D. Nosetto, Y. Nouvellon, M. A. Nuñez, R. Ogaya, J. Ogée, J. Okello, J. Olejnik, J. E. Olesen, H. Opedal, S. Orsenigo, A. Palaj, T. Pampuch, A. V. Panov, M. Pärtel, A. Pastor, A. Pauchard, H. Pauli, M. Pavelka, W. D. Pearse, M. Peichl, L. Pellissier, R. M. Penczykowski, J. Penuelas, M. Petit Bon, A. Petraglia, S. S. Phartyal, G. K. Phoenix, C. Pio, A. Pitacco, C. Pitteloud, R. Plichta, F. Porro, M. Portillo-Estrada, J. Poulenard, R. Poyatos, A. S. Prokushkin, R. Puchalka, M. Puşcaş, D. Radujković, K. Randall, A. Ratier Backes, S. Remmele, W. Remmers, D. Renault, A. C. Risch, C. Rixen, S. A. Robinson, B. J. Robroek, A. V. Rocha, C. Rossi, G. Rossi, O. Roupsard, A. V. Rubtsov, P. Saccone, C. Sagot, J. Sallo Bravo, C. C. Santos, J. M. Sarneel, T. Scharnweber, J. Schmeddes,

M. Schmidt, T. Scholten, M. Schuchardt, N. Schwartz, T. Scott, J. Seeber, A. C. Segalin de Andrade, T. Seipel, P. Semenchuk, R. A. Senior, J. M. Serra-Diaz, P. Sewerniak, A. Shekhar, N. V. Sidenko, L. Siebicke, L. Siegwart Collier, E. Simpson, D. P. Siqueira, Z. Sitková, J. Six, M. Smiljanic, S. W. Smith, S. Smith-Tripp, B. Somers, M. V. Sørensen, J. J. L. Souza, B. I. Souza, A. Souza Dias, M. J. Spasojevic, J. D. Speed, F. Spicher, A. Stanisci, K. Steinbauer, R. Steinbrecher, M. Steinwandter, M. Stemkovski, J. G. Stephan, C. Stiegler, S. Stoll, M. Svátek, M. Svoboda, T. Tagesson, A. J. Tanentzap, F. Tanneberger, J. P. Theurillat, H. J. Thomas, A. D. Thomas, K. Tielbörger, M. Tomaselli, U. A. Treier, M. Trouillier, P. D. Turtureanu, R. Tutton, V. A. Tyystjärvi, M. Ueyama, K. Ujházy, M. Ujházyová, D. Uogintas, A. V. Urban, J. Urban, M. Urbaniak, T. M. Ursu, F. P. Vaccari, S. Van de Vondel, L. van den Brink, M. Van Geel, V. Vandvik, P. Vangansbeke, A. Varlagin, G. F. Veen, E. Veenendaal, S. E. Venn, H. Verbeeck, E. Verbrugggen, F. G. Verheijen, L. Villar, L. Vitale, P. Vittoz, M. Vives-Ingla, J. von Oppen, J. Walz, R. Wang, Y. Wang, R. G. Way, R. E. Wedegärtner, R. Weigel, J. Wild, M. Wilkinson, M. Wilmking, L. Wingate, M. Winkler, S. Wipf, G. Wohlfahrt, G. Xenakis, Y. Yang, Z. Yu, K. Yu, F. Zellweger, J. Zhang, Z. Zhang, P. Zhao, K. Ziemblińska, R. Zimmermann, S. Zong, V. I. Zyryanov, I. Nijs, and J. Lenoir. Global maps of soil temperature. *Global Change Biology*, 28(9):3110–3144, May 2022. ISSN 13652486. doi: 10.1111/gcb.16060. Publisher: John Wiley and Sons Inc.

S. Lundberg and S.-I. Lee. A Unified Approach to Interpreting Model Predictions, Nov. 2017. URL http://arxiv.org/abs/1705.07874. arXiv:1705.07874 [cs, stat].

K. G. MacDicken. Global Forest Resources Assessment 2015: What, why and how? *Forest Ecology and Management*, 352:3–8, 2015. ISSN 03781127. doi: 10.1016/j.foreco.2015.02.006. URL http://dx.doi.org/10.1016/j.foreco.2015.02.006. Publisher: Elsevier B.V.

A. Mamalakis, I. Ebert-Uphoff, and E. Barnes. Explainable Artificial Intelligence in Meteorology and Climate Science: Model Fine-Tuning, Calibrating Trust and Learning New Science. In A. Holzinger, R. Goebel, R. Fong, T. Moon, K.-R. Müller, and W. Samek, editors, *xxAI - Beyond Explainable AI*, volume 13200, pages 315–339. Springer International Publishing, Cham, 2022. ISBN 978-3-031-04082-5 978-3-031-04083-2. doi: 10.1007/978-3-031-04083-2_16. URL https://link.springer.com/10.1007/978-3-031-04083-2_16. Series Title: Lecture Notes in Computer Science.

G. Matasci, T. Hermosilla, M. A. Wulder, J. C. White, N. C. Coops, G. W. Hobart, D. K. Bolton, P. Tompalski, and C. W. Bater. Three decades of forest structural dynamics over Canada's forested ecosystems using Landsat time-series and lidar plots. *Remote Sensing of Environment*, 216:697–714, Oct. 2018. ISSN 00344257. doi: 10.1016/j.rse.2018.07.024. Publisher: Elsevier Inc.

H. D. Matthews, N. P. Gillett, P. A. Stott, and K. Zickfeld. The proportionality of global warming to cumulative carbon emissions. *Nature*, 459(7248):829–832, 2009. ISSN 00280836. doi: 10.1038/nature08047. Publisher: Nature Publishing Group.

H. D. Matthews, K. Zickfeld, M. Dickau, A. J. MacIsaac, S. Mathesius, C.-M. Nzotungicimpaye, and A. Luers. Temporary nature-based carbon removal can lower peak warming in a well-below 2 °C scenario. *Communications Earth & Environment*, 3(1):1–8, 2022. doi: 10.1038/s43247-022-00391-z. Publisher: Springer US.

M. B. Mills, Y. Malhi, R. M. Ewers, L. K. Kho, Y. A. Teh, S. Both, D. F. Burslem, N. Majalap, R. Nilus, W. Huaraca Huasco, R. Cruz, M. M. Pillco, E. C. Turner, G. Reynolds, and T. Riutta. Tropical forests post-logging are a persistent net carbon source to the atmosphere. *Proceedings of the National Academy of Sciences of the United States of America*, 120(3), Jan. 2023. ISSN 10916490. doi: 10.1073/pnas.2214462120. Publisher: NLM (Medline).

J. Muñoz-Sabater, E. Dutra, A. Agustí-Panareda, C. Albergel, G. Arduini, G. Balsamo, S. Boussetta, M. Choulga, S. Harrigan, H. Hersbach, B. Martens, D. G. Miralles, M. Piles, N. J. Rodríguez-Fernández, E. Zsoter, C. Buontempo, and J. N. Thépaut. ERA5-Land: A state-of-the-art global reanalysis dataset for land applications. *Earth System Science Data*, 13(9):4349–4383, Sept. 2021. ISSN 18663516. doi: 10.5194/essd-13-4349-2021. Publisher: Copernicus Publications.

T. Nguyen, J. Brandstetter, A. Kapoor, J. K. Gupta, and A. Grover. ClimaX: A foundation model for weather and climate. *arXiv*, Jan. 2023. URL http://arxiv.org/abs/2301.10343. arXiv: 2301.10343.

T. J. Osborn, S. C. Raper, and K. R. Briffa. Simulated climate change during the last 1,000 years: Comparing the ECHO-G general circulation model with the MAGICC simple climate model. *Climate Dynamics*, 27(2-3):185–197, Aug. 2006. ISSN 09307575. doi: 10.1007/s00382-006-0129-5.

Y. Pan, R. A. Birdsey, J. Fang, R. Houghton, E. Pekka, W. A. Kurz, O. L. Phillips, A. Shvidenko, S. L. Lewis, G. Canadell, P. Ciais, R. B. Jackson, S. W. Pacala, A. D. Mcguire, S. Piao, A. Rautiainen, S. Sitch, and D. Hayes. A Large and Persistent Carbon Sink in the World's Forests. *Science*, 333, 2011. doi: 10.1126/science.1201609.

C. Pappas, J. Maillet, S. Rakowski, J. L. Baltzer, A. G. Barr, T. A. Black, S. Fatichi, C. P. Laroque, A. M. Matheny, A. Roy, O. Sonnentag, and T. Zha. Aboveground tree growth is a minor and decoupled fraction of boreal forest carbon input. *Agricultural and Forest Meteorology*, 290(December 2019):108030, 2020. ISSN 01681923. doi: 10.1016/j.agrformet.2020.108030. URL https://doi.org/10.1016/j.agrformet.2020.108030. Publisher: Elsevier.

J. Pongratz, C. Schwingshackl, S. Bultan, W. Obermeier, F. Havermann, and S. Guo. Land Use Effects on Climate: Current State, Recent Progress, and Emerging Topics. *Current Climate Change Reports*, 7(4):99–120, 2021. ISSN 21986061. doi: 10.1007/s40641-021-00178-y. URL https://doi.org/10.1007/s40641-021-00178-y. Publisher: Springer International Publishing ISBN: 0123456789.

S. Rasp, M. S. Pritchard, and P. Gentine. Deep learning to represent subgrid processes in climate models. *Proceedings of the National Academy of Sciences*, 115(39): 9684–9689, Sept. 2018. ISSN 0027-8424, 1091-6490. doi: 10.1073/pnas.1810286115. URL https://pnas.org/doi/full/10.1073/pnas.1810286115.

E. D. Schulze, R. Valentini, and O. Bouriaud. The role of net ecosystem productivity and of inventories in climate change research: the need for "net ecosystem productivity with harvest", NEPH. *Forest Ecosystems*, 8(1):15, Mar. 2021. ISSN 2197-5620. doi: 10.1186/s40663-021-00294-z. URL https://doi.org/10.1186/s40663-021-00294-z.

C. J. Smith, P. M. Forster, M. Allen, N. Leach, R. J. Millar, G. A. Passerello, and L. A. Regayre. FAIR v1.3: A simple emissions-based impulse response and carbon cycle model. *Geoscientific Model Development*, 11(6):2273–2297, June 2018. ISSN 19919603. doi: 10.5194/gmd-11-2273-2018. Publisher: Copernicus GmbH.

C. Sothe, A. Gonsamo, J. Arabian, W. A. Kurz, S. A. Finkelstein, and J. Snider. Large Soil Carbon Storage in Terrestrial Ecosystems of Canada. *Global Biogeochemical Cycles*, 36(2):1–18, 2022. ISSN 19449224. doi: 10.1029/2021GB007213.

M. Sundararajan, A. Taly, and Q. Yan. Axiomatic Attribution for Deep Networks. *arXiv*, Mar. 2017. URL http://arxiv.org/abs/1703.01365. arXiv: 1703.01365.

T. Tagesson, G. Schurgers, S. Horion, P. Ciais, F. Tian, M. Brandt, A. Ahlström, J. P. Wigneron, J. Ardö, S. Olin, L. Fan, Z. Wu, and R. Fensholt. Recent divergence in the contributions of tropical and boreal forests to the terrestrial carbon sink. *Nature Ecology and Evolution*, 4(2):202–209, 2020. ISSN 2397334X. doi: 10.1038/s41559-019-1090-0. URL http://dx.doi.org/10.1038/s41559-019-1090-0. Publisher: Springer US.

W. S. Walker, S. R. Gorelik, S. C. Cook-Patton, A. Baccini, M. K. Farina, K. K. Solvik, P. W. Ellis, J. Sanderman, R. A. Houghton, S. M. Leavitt, C. R. Schwalm, and B. W. Griscom. The global potential for increased storage of carbon on land. *PNAS*, 2022. doi: 10.1073/pnas. URL https://doi.org/10.1073/pnas.2111312119.

J. A. Wang, A. Baccini, M. Farina, J. T. Randerson, and M. A. Friedl. Disturbance suppresses the aboveground carbon sink in North American boreal forests. *Nature Climate Change*, 11(May), 2021.

D. Watson-Parris. Machine learning for weather and climate are worlds apart. *Philosophical Transactions of the Royal Society A: Mathematical, Physical and Engineering Sciences*, Aug. 2020. doi: 10.1098/rsta.2020.0098. URL http://arxiv.org/abs/2008.10679. arXiv: 2008.10679.

D. Watson-Parris, Y. Rao, D. Olivié, Seland, P. Nowack, G. Camps-Valls, P. Stier, S. Bouabid, M. Dewey, E. Fons, J. Gonzalez, P. Harder, K. Jeggle, J. Lenhardt, P. Manshausen, M. Novitasari, L. Ricard, and C. Roesch. ClimateBench v1.0: A Benchmark for Data-Driven Climate Projections. *Journal of Advances in Modeling Earth Systems*, 14(10), Oct. 2022. ISSN 1942-2466, 1942-2466. doi: 10.1029/2021MS002954. URL https://onlinelibrary.wiley.com/doi/10.1029/2021MS002954.

E. B. Wiken, D. Gauthier, I. Marshall, K. Lawton, and H. Hirvonen. Perspective on Canada's Ecosystems: An Overview of the Terrestrial and Marine Ezones Prepared for the Canadian Council on Ecological Areas Ottawa, Ontario. Technical report, Agriculture and Agri-Food Canada, 1996.

M. A. Wulder, T. Hermosilla, J. C. White, and N. C. Coops. Biomass status and dynamics over Canada's forests: Disentangling disturbed area from associated aboveground biomass consequences. *Environmental Research Letters*, 15(9), Sept. 2020. ISSN 17489326. doi: 10.1088/1748-9326/ab8b11. Publisher: IOP Publishing Ltd.

Appendix A

Appendix

The efforts described in this Appendix use the managed forest as a study area - I initially thought I would be best to consider the area where wood harvest occurred, but this definition and boundary changes year to year depending on the extent of wood harvest. Using Canada's ecozones provided more comparability with other studies and a much more stable boundary. I initially trained the LSTM on all ecozones, including marine and arctic areas. This was unable to be learned by the model as there was too much difference between the data between ecozones. Creating a model architecture that took this into consideration, such as multi-task learning, could be an interesting avenue of research.

Before working with an LSTM, I attempted to use fully-connected neural network (also known as an artificial neural network or multi-layer perceptron) to make the carbon stock estimations. This model architecture is not temporally aware and only considered a single year and grid cell at a time. This cause the model to have very noisy predictions over the study period, but enabled a much longer inference period. Because 30 of the 35 years of observable data were not being used as time series input, all 35 years could be used for inference. We can see in Figure A.1 there is an extreme amount of variability, with total carbon stocks fluctuating by thousands of Mt C year to year. As the data is yearly averages, there can be some variation year to year and this was misleading for the neural network. It necessitated taking a longer "image" of the climate at a particular grid cell, to better teach the neural network the local climate.

Figure A.2 Shows the predictions based on the reforestation scenario. Here we can again see large variation year to year and a negative contribution on the last year, which should not be the case when adding tree cover.

Finally, in Figure A.3 we can see the spatial distribution of predictions made for the year 2013. As discussed in the Supplemental Material of the manuscript, the LSTM did not perform well at predicting variability in the carbon store. This model was even less able to predict variation, as we can see the only substantial areas with little carbon are areas with almost no tree cover (the area spanning the southern parts of Alberta, Saskatchewan and Manitoba).

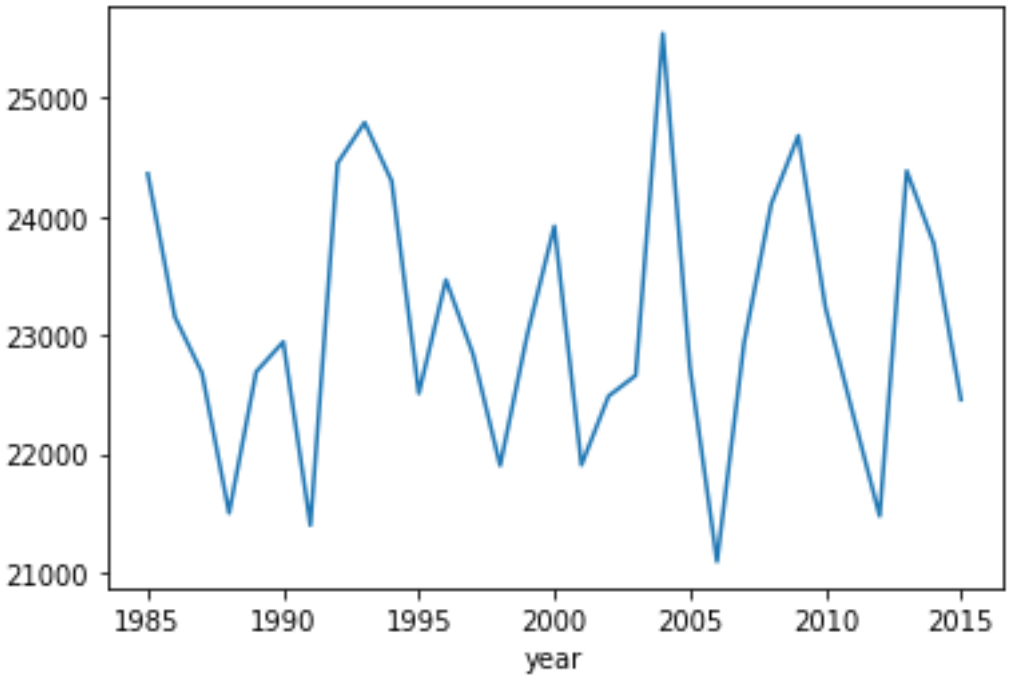

FIGURE A.1: Predictions of total carbon in Canada's managed forest using the fully-connected neural network.

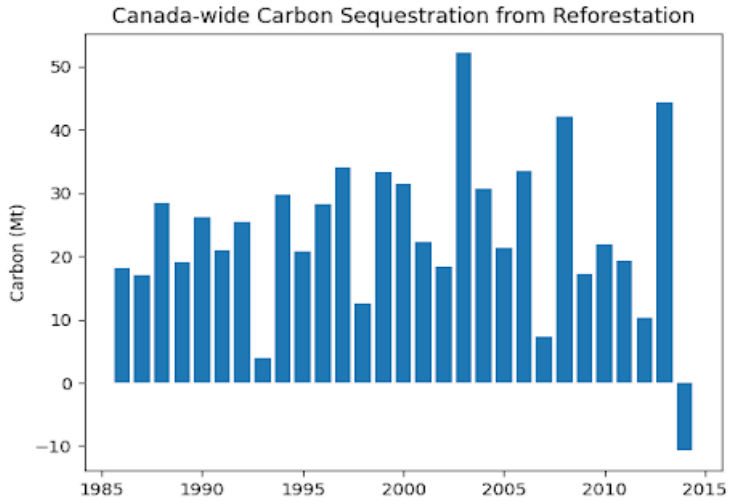

FIGURE A.2: Predictions of total carbon with reforestation dataset using the fully-connected neural network.

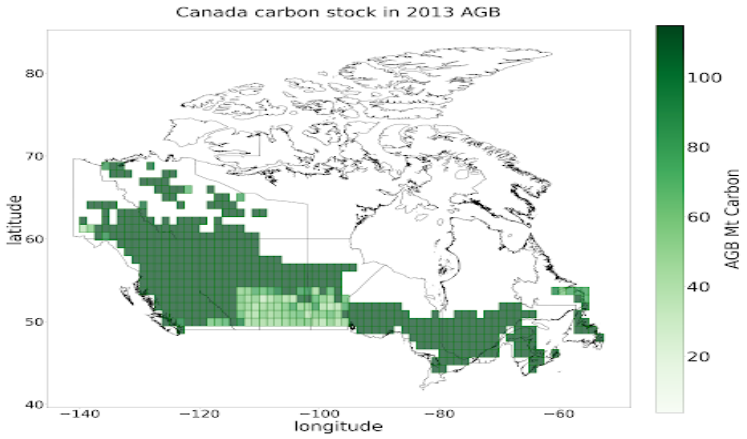

FIGURE A.3: Spatial distributions of carbon predictions for the year 2013 using the fully-connected neural network.